Energy Advances

ROYAL SOCIETY OF CHEMISTRY

REVIEW ARTICLE

View Article Online
View Journal | View Issue



Cite this: *Energy Adv.*, 2024, 3, 1144

# Recent advancements in catalyst coated membranes for water electrolysis: a critical review

Rajangam Vinodh, * Tamilazhagan Palanivel, Shankara Sharanappa Kalanur and Bruno G. Pollet *

Received 1st March 2024,
Accepted 5th May 2024

DOI: 10.1039/d4ya00143e

rsc.li/energy-advances

It is imperative to transition towards sustainable energy sources to mitigate the escalating threat of global warming and ameliorate the adverse impacts of climatic changes. Water electrolysis (WE) stands out as a promising pathway for producing green hydrogen among various renewable energy technologies. Hydrogen offers a flexible and eco-friendly energy solution that holds promise for reducing carbon emissions across multiple industries. Recent progress in sustainable hydrogen production reflects its ability to meet the growing need for clean fuel and efficient energy storage. Despite the myriad components influencing the efficacy and long-term stability of electrolysis systems, the catalyst coated membrane (CCM) assumes a pivotal role. This present review comprehensively examines the state-of-the-art in catalyst coated membrane technology for water electrolysis, elucidating fabrication techniques, design principles, durability, degradation mechanisms and performance-enhancing strategies. Furthermore, this review article contributes to further technological advancements and future perspectives of CCM in water electrolysers, focusing on electrolyser design, materials innovation, and system integration for commercially viable hydrogen production purposes.

*Green Hydrogen Lab (GH2Lab), Hydrogen Research Institute (HRI), Université du Québec à Trois-Rivières (UQTR), 3351 Boulevard des Forges, Trois-Rivières, QC G9A 5H7, Canada. E-mail: Vinodh.Rajangam@uqtr.ca, Bruno.Pollet@uqtr.ca*

**Rajangam Vinodh**

*Rajangam Vinodh have been working as a post-doctoral researcher at IRH, UQTR since May 2022. He completed his bachelor's and master's degree in chemistry from the University of Madras, Tamil Nadu, India in 2002 and 2005, respectively. He graduated with a PhD, from Anna University, India (2012) and his research field was fabrication of membrane electrode assembly for alkaline membrane fuel cell application. After his PhD, he was selected as Assistant Professor (2013 to 2018) at Hanseo University, South Korea. In 2018, he was appointed as a Post-Doctoral Researcher (April 2018 to April 2022) at Pusan National University, South Korea. He is expert in electrochemical workstations and the fabrication of energy storage systems such as solid-state asymmetric supercapacitors, fuel cells, and $CO_2$ adsorption. To date, he has authored 115 international publications in well-reputed journals, 5 book chapters and presented his research findings in 63 national/international conferences all around the globe including Germany, Japan, Singapore, South Korea, India, China, Bangkok and Nepal. Further, he is serving as a scientific reviewer for more than 30 international journals.*

**Tamilazhagan Palanivel**

*Tamilazhagan Palanivel is currently pursuing his PhD in Energy and Materials Science at the University of Quebec at Trois-Rivières (UQTR), supervised by Prof. Bruno G. Pollet. He completed his Bachelor's and Master's degrees in Polymer Science and Engineering at Anna University, Chennai, India, in 2018 and 2021, respectively. His research primarily revolves around the development of Ion exchange membranes, with a particular focus on facilitating green hydrogen production.*

# 1. Introduction

The global dependence on fossil fuels for energy generation has led to considerable environmental impacts, prompting the need for a transition to cleaner and sustainable energy sources. Hydrogen has emerged as a crucial energy carrier offering potential solutions to the energy-related issues. With its high energy density per unit mass (33.3 kW h $kg^{-1}$) and zero emission upon combustion, hydrogen represents an ideal renewable energy option, serving as a feasible alternative to traditional hydrocarbons.[1] Moreover, the transition towards the hydrogen-based infrastructure and economy holds the promise of environmental advantages, despite facing certain obstacles, which are overshadowed by the drawbacks associated with continuing reliance on hydrocarbon fuels.[2] The favourable characteristics of a hydrogen economy have garnered considerable attention from stakeholders, spurring dedicated efforts from scientists and researchers across various domains to advance hydrogen technologies.

Currently, numerous hydrogen generation strategies rely on technologies that utilize fossil fuels (such as coal, petroleum, and natural gas), resulting in the emission of greenhouse gases (GHGs). These processes yield both ''grey hydrogen'' and ''blue hydrogen'', with the latter incorporating carbon sequestration measures. Given the pressing environmental concerns, there is a critical need to prioritize $H_2$ manufacture technologies that are well-organized, almost zero emission, and ecologically sustainable. In this regard, green $H_2$ production through renewable energy-powered water electrolysis stands out as a compelling solution, as it circumvents $CO_2$ emissions, aligning with sustainability and environmental conservation goals.[3–8] Furthermore, water electrolysis technologies facilitate the storage of intermittent energy from renewable sources in the form of hydrogen, enabling on-demand utilization.

# 2. Water electrolyser types

Water electrolysis is a widely well-established technology for converting water into hydrogen ($H_2$) and oxygen ($O_2$).[9–12] Electrolysis is categorized according to the opted setup including type of electrolyte employed in the electrolyser. Common electrolyser types comprise alkaline water electrolysers (AWE), proton exchange membrane water electrolysers (PEMWE),[13] anion exchange membrane water electrolysers (AEMWE),[14] and solid oxide electrolysers (SOE).[15,16] Fig. 1 illustrates the graphical representation of the above-mentioned water electrolysers and their operating mechanism.

## 2.1. Alkaline water electrolysis (AWE)

In alkaline water electrolysis (Fig. 1(a)), nickel-based materials are commonly used at the anode, and cobalt-based oxides are

**Shankara Sharanappa Kalanur**

*Shankara Sharanappa Kalanur is currently working as a research head at Pollet's group and as a researcher officer at hydrogen research institute, UQTR (since October 2022). Previously, he worked as a assistant Professor at Ajou university, South Korea and as a visiting scientist at Korea institute of science and technology. Dr Shankara Kalanur is an expert in hydrogen production technology (electrolysis, PEC water splitting and methane pyrolysis), electrochemistry, hydrogen sensors, electrochemical sensors, solar cells, and energy storage devices. He has procured scientific research funding's ($ 800 000 total) via several projects to develop electrode materials for sustainable and renewable hydrogen energy production and sensors. His aptitude to articulate complex ideas to both technical and non-technical audiences have resulted in 85 publications, 6 US patents, 12 Korean Patents, 4 technology transfers to companies, 4 book chapters, 2 research projects (funded by Korea research foundation), and 4 conference presentations.*

**Bruno G. Pollet**

*Bruno G. Pollet has both a strong international industrial and academic experience. He has worked on Hydrogen Energy in the UK, Japan, South Africa, Norway, and Canada. He is a Fellow of the UK Royal Society of Chemistry, and a Professor of Chemistry at the University of Quebec at Trois-Rivières (UQTR) in Canada. Since 2022, he is a member of the Council of Engineers for the Energy Transition: An Independent Advisory Council to the United Nations' Secretary-General. He has recently been awarded the prestigious NSERC Canada Research Chair Tier 1 in Green Hydrogen Production with a strong focus on the next generation of electrolysers. Since February 2023, he is also Director of the UQTR Institute for Hydrogen Research (IHR), Director of the Green Hydrogen Laboratory (GH2Lab), Adjunct Professor of Renewable Energy at the Department of Energy & Process Engineering (DEPE), Norwegian University of Science and Technology (NTNU), Adjunct Professor at the Hydrogen Safety Engineering Research (HySAFER), Ulster University (UK) and President of the Green Hydrogen Division of the International Association for Hydrogen Energy (IAHE). In 2022, the hydrogen community awarded him with the ''IAHE Sir William Grove Award'' for his work in hydrogen, fuel cell and electrolyser technologies by the IAHE. He is also member of the Board of Directors of the Canadian Hydrogen and Fuel Cell Association (CHFCA) and Hydrogen Québec.*

favoured for the cathode. Typically, the preferred liquid electrolyte consists of 30–40% KOH.[17,18] This electrolyte is distributed *via* the electrodes to maintain the essential electrolysis conditions. A porous diaphragm is employed to separate the anode and cathode chambers, allowing the passage of hydroxyl ions ($OH^-$) while preventing the escape of $H_2$ and $O_2$ gases.[17,19,20] Diaphragms are typically made from materials such as ceramic oxides (*e.g.*, asbestos and potassium titanate) or polymers (*e.g.*, polypropylene (PP) and polyphenylene sulphide (PPS)).[21–24] AWE usually functions at a current density of around 400 mA $cm^{-2}$, at moderate temperatures between 70 and 90 °C, with a polarization voltage ranging from 1.85 to 2.2 V, and conversion efficiencies ranging from 60 to 80%.[25] The advantages of AWE include its ability to produce hydrogen without requiring noble-metal catalysts and its ease of operation at relatively low temperatures.[26]

### 2.2. Proton exchange membrane water electrolysis (PEMWE)

In PEM water electrolysis (depicted in Fig. 1(b)), iridium dioxide ($IrO_2$) and platinum (Pt) black serve as catalysts for oxidation and reduction of water molecules at the anode and cathode, respectively.[27,28] However, instead of a liquid electrolyte, an acidic membrane, like Nafion® from DuPont is employed as a solid electrolyte between the anode and cathode sides. The membrane facilitates the conduction of $H^+$ ions from the anode to the cathode, effectively segregating the $H_2$ and $O_2$ generated during the reaction while maintaining the potential difference. PEM electrolysers can achieve a current density of 2000 mA $cm^{-2}$ at 90 °C, with a voltage of around 2.1 V.[29] The kinetics of the $H_2$ and $O_2$ production reaction in PEMWE surpasses those of alkaline electrolysis, mainly because of the acidic electrolyte and the metallic surface of the electrodes yielding high purity hydrogen (without the use of dryers).[30] PEM electrolysis offers improved safety by eliminating the need for caustic electrolytes.[31] Notably, PEM electrolysis allows for high-pressure operation on the cathode side, whereas the anode can operate at atmospheric pressure.[32]

### 2.3. Anion exchange membrane water electrolysis (AEMWE)

AEMWE technology represents the latest advancement in water electrolysis, driven primarily by electrochemical applications for hydrogen production in recent years. AEMWE combines the advantages of both alkaline and PEM water electrolysers[33] providing a balanced solution for hydron production. The schematic working mechanism of an AEMWE is depicted in Fig. 1(c), where $H^+$ and $OH^-$ ions are generated at the cathode side. Additionally, non-noble catalyst materials can be employed for AEMWEs, leading to reduced hydrogen production prices.[34] Nevertheless, the performance of AEM still encounters challenges owing to inadequate catalyst activity and inferior ionic conductivity. Consequently, further investigations are necessary for AEMWE, particularly regarding membrane durability, cell cost, and efficiency.[35,36] Recently, several commercial provides have emerged to offer AEMWE systems indicating the technology readiness of the AEM electrolysis methods.

### 2.4. Solid oxide electrolysis cell (SOEC)

SOEC has attracted significant attention from researchers for its capacity to convert electrical energy into chemical energy while yielding ultra-pure $H_2$ with enhanced yield.[37,38] Operating

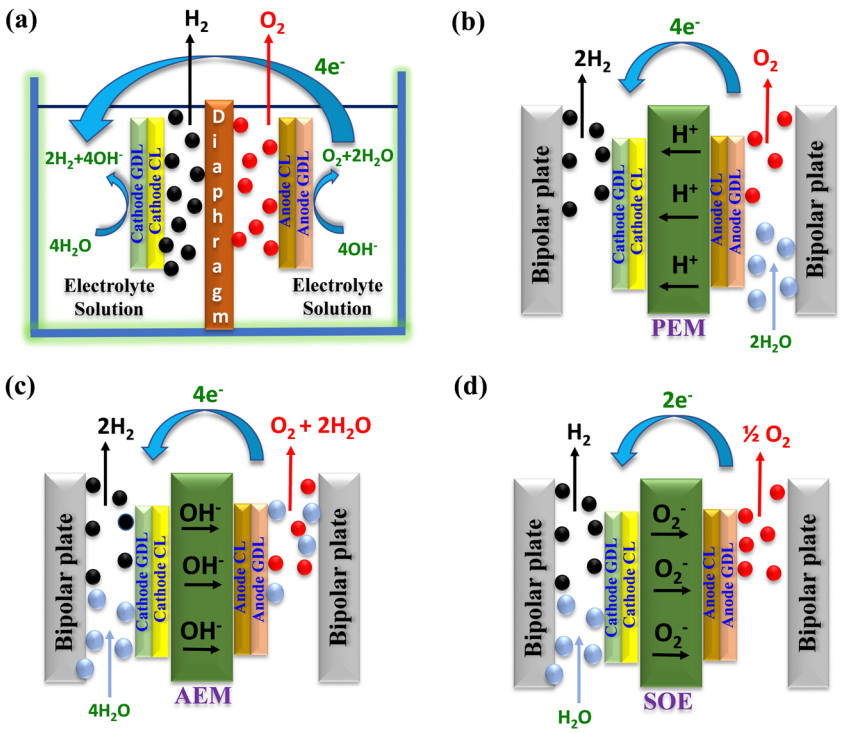


Fig. 1 Schematic illustration of the different electrolysis techniques: (a) AWE, (b) PEMWE, (c) AEMWE, and (d) SOE.

Table 1 Recent review articles based on water electrolysis published in scientific journals

| S. no. | Title and highlights of the review article | Published year | Ref. |
|---|---|---|---|
| 1 | Hydrogen production by water electrolysis technologies: a review<br>• The state-of-the-art of impure water electrolysis was assessed<br>• The available water electrolysis system was compared<br>• A whole system was investigated to cover pure water and power demand using sea water | 2023 | 42 |
| 2 | Recent review and evaluation of green hydrogen production *via* water electrolysis for a sustainable and clean energy society<br>• WE process and their techno-commercial prospects were discussed<br>• Recent developments in electrode and photoelectrode materials were summarized<br>• An environmental aspect of green hydrogen was summarized<br>• Case studies in various countries related to green hydrogen were also discussed | 2024 | 43 |
| 3 | Technical evaluation of the flexibility of water electrolysis systems to increase energy flexibility: a review<br>• Overview of the current state of the art in the operation of electrolysis systems<br>• Summarized collection of flexibility parameters to compare electrolysis systems<br>• Introduction of modularization in electrolysis systems for orchestration | 2023 | 44 |
| 4 | Mechanism analyses and optimization strategies for performance improvement in low-temperature water electrolysis systems *via* the perspective of mass transfer: a review<br>• The mass transfer mechanism on the WE process is illustrated<br>• Optimization ideas improving mass transfer in PEMWE cells are summarized<br>• Methods of reducing gas cross-over and a detailed review of bubble effects are discussed | 2023 | 45 |
| 5 | Electrocatalysts for alkaline water electrolysis at ampere-level current densities: a review<br>• Electrocatalyst for AWE at ampere-current densities<br>• Experimental conditions need to be reconsidered to accurately assess the performance of electrocatalysts<br>• Charge transfer, mass transport, *in situ* reconstruction, gas bubble effect, and electrochemical corrosion are elaborated | 2024 | 46 |
| 6 | Overview of alkaline water electrolysis modeling<br>• Current research focuses and the direction of AWE modeling<br>• Electrochemical effects, heat, mass transfer, and two-phase flow effect of the model are summarized | 2024 | 47 |
| 7 | Review and prospects of PEM water electrolysis at elevated temperature operation<br>• An examination of the materials and cell components employed in high-temperature PEMWE operations under both liquid and steam conditions in provided<br>• The experimental modeling results documented thus far underscore the forthcoming challenges and indicate areas discussed | 2024 | 48 |
| 8 | Review of next-generation hydrogen production from offshore wind using water electrolysis<br>• The impact of power from fluctuating offshore wind on electrolyser performance was discussed<br>• Materials and scale-up influence the electrolyser choice for offshore wind was illustrated | 2024 | 49 |
| 9 | Recent advances in hydrogen production through proton exchange membrane water electrolysis – a review<br>• Different WE techniques and their technical specifications were briefly summarized from a commercial perspective<br>• Focused on PEMWE cell components (membranes, GDLs, bipolar plates, and electrocatalysts) | 2023 | 50 |
| 10 | Key components and design strategy of the membrane electrode assembly for alkaline water electrolysis<br>• Reviewed state-of-the-art MEAs, which include electrocatalysts, membranes, and gas/liquid diffusion layers, as well as the current development in MEA fabrication methods | 2023 | 51 |
| 11 | Green hydrogen production by anion exchange membrane water electrolysis: status and future perspectives<br>• Various types of WE systems are briefly discussed<br>• State-of-the-art AEMWE topics, such as membrane, catalysts development, and stability were discussed | 2023 | 52 |
| 12 | Recent advancements of polymeric membranes in anion exchange membrane water electrolyser (AEMWE): a critical review<br>• Recent achievements and advancements of AEMWE in terms of anion exchange membranes, AEM degradation mechanism, and the electrocatalyst design have been discussed | 2023 | 53 |
| **13** | **Recent advancement of catalyst coated membrane for water electrolysis: a critical review**<br>**• The state-of-the-art catalyst coated membrane was thoroughly examined**<br>**• Various components influencing the efficiency and durability of the WE system are illustrated**<br>**• Future technological advancements and future perspectives of CCM in WE in terms of electrolyser design, materials innovation, and system integration are depicted** | **2024** | **[This article]** |

at high pressure and temperatures ranging from 500 to 850 °C, SOEC releases water in the form of steam. Typically, SOEC utilizes $O_2^-$ conductors, often comprising of nickel/yttria-stabilized zirconia,[39] as depicted in Fig. 1(d). One prominent advantage of the SOE method is its ability to function at elevated temperatures, which offers distinct benefits compared to low-temperature water electrolysis techniques. However, solid oxide electrolysis methods pose several concerns regarding durability and efficiency that must be addressed before pilot-scale production and commercialization.[40,41]

## 3. Recent reviews on water electrolysis

Table 1 presents a comprehensive overview of recent review articles published in well-reputed journals focusing on various aspects of the water electrolysis phenomenon. Mostafa El-Shafie provided insights into the state-of-the-art technologies capable of utilizing contaminated water in WE systems.[42] N. S. Hassan *et al.* delved into the water electrolysis process and its techno-commercial prospects, including case studies from various countries related to green hydrogen production.[43] Hannes Lange *et al.* discussed the collection of flexibility parameters for comparing and introducing modularization in electrolysis systems for orchestration purposes.[44] Hong Lv *et al.* deliberated the mechanism of mass transfer in the WE process, optimization concepts to enhance mass transfer in PEMWE cells, and methods for reducing gas cross-over.[45]

Zehua Zou *et al.* highlighted the encounters and outlook of electrocatalysts for ampere-level AWE, focusing on parameters such as accelerating charge transfer, improving mass transport, justifying gas bubble effect, observing reconstruction procedure, and enhancing corrosion resistance in electrocatalyst design.[46] Camilia Daoudi and Tijani Bounahmidi provided a comprehensive review of recent research studies in AWE modelling.[47] Marco Bonanno *et al.* discussed the prospects of PEMWE at elevated temperature (<90 °C) operation.[48] Daniel Niblett *et al.* reviewed next-generation $H_2$ production from offshore wind employing the WE system.[49] S. Shiva Kumar and Hankwon Kim predominantly focused on recent advances in hydrogen production through the PEMWE system, highlighting effective results and identifying research cracks and encounters for cost reduction and industrialization.[50]

Lei Wan *et al.* reviewed the fundamentals of AEMWE, covering the current state of MEAs, membranes, electrocatalysts, and preparation strategies of MEA.[51] Daniela S. Falcão discussed new materials (anion exchange membranes, electrocatalysts, MEA design) and provided future directions to enhance AEMWE technology.[52] Rajangam Vinodh *et al.* elucidated recent advancements in various anion exchange membranes in AEMWE, focusing on ionic conductivity, the degradation mechanism of AEM, and electrocatalyst design.[53]

While the above review articles offer valuable insights, they predominantly focus on the improvement of various technologies and techno-economic analysis for hydrogen production, often neglecting environment assessments and material utilization. To the best of the authors' knowledge, there are no comprehensive review articles explaining recent advancements in CCMs for water electrolysis. Hence, this present review provides an in-depth exploration of the current state-of-the-art catalyst coated membranes in WE, offering insights into their design principles, fabrication methodologies, and the intrinsic interplay between materials and the electrochemical process.

## 4. Components of water electrolysis

Typically, in membrane based (in PEM/AEM) water electrolysis stacks, several components are integrated, including a membrane, electrode materials (consisting of catalyst layers (CLs)/electrocatalysts), gas diffusion layers (GDLs)/porous transport layers (PTLs), bipolar plates/separator plates, current collectors/end plates, as depicted in Fig. 2.[37,54,55] At the core of WE systems lies the membrane–electrode assembly (MEA), which plays a crucial role as the site of electrochemical reactions. The MEA features a layered structure comprising an ion

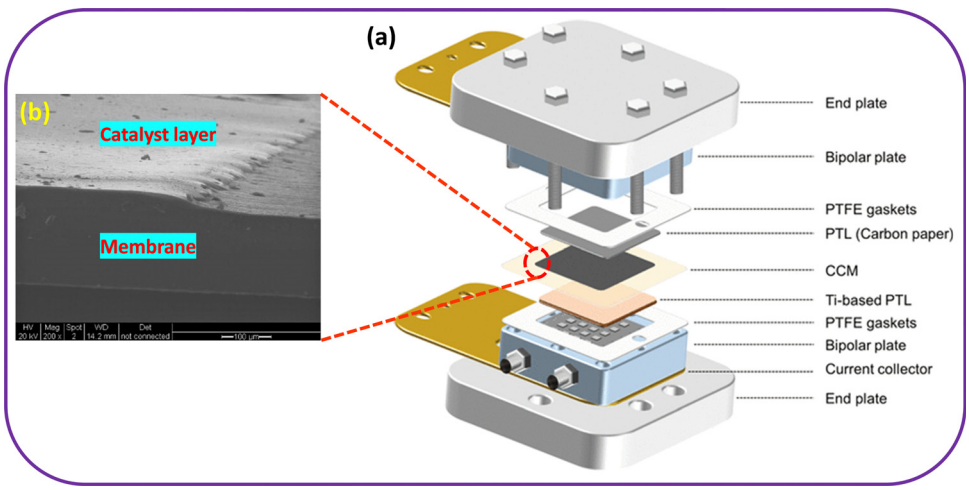


Fig. 2 (a) Schematic look of the PEM water electrolyser components and (b) zoomed view of CCM. Reproduced with permission from ref. 54 and 37. Copyright 2021, ACS and copyright 2010, Elsevier.

exchange membrane (IEM) and a pair of OER/HER electrodes, consisting of catalysts, and supporting materials. Depending on the specific application, the IEM can be either an anion exchange membrane or a PEM, regulating ion transport selectivity. The GDL aids as a scaffold for catalysts, assisting the transportation of liquid and gaseous products as well as charge carriers.[56] The MEA design considerably influences catalyst utilization and the necessary electrolyte concentration to maintain high system efficiency. Consequently, the quality of MEAs directly impacts the performance, price, and stability of ensuing WE systems. Hence, achieving mass production of high-quality MEAs is crucial for the marketable implementation of this technology. In WE technology, two primary MEA production methods have emerged: (i) the catalyst coated substrate (CCS, also referred to as a catalyst-coated electrode),[57–60] and (ii) the catalyst coated membrane (CCM).[61] A detailed comparison between CCS and CCM is provided in Table 2.

In summary, both the CCM and CCS configurations have their own merits and demerits in water electrolysers. The selection between these two approaches depends on various factors such as performance requirements, cost considerations, and operational limitations. However, the CCM method addresses certain challenges associated with the CCS strategy by ensuring optimal catalyst contact with the membrane, thereby enhancing process efficiency and enabling different catalyst utilization, leading to lower catalyst loading.[62,63] Additionally, the polarization and ohmic resistances between the catalyst layer and the membrane can be mitigated; eventually enhancing the performance of CCM-based MEAs. Furthermore, CCM configurations offer benefits in terms of mass transport, specific power, and cell efficiency, while CCS configuration provides advantages in mechanical stability, catalyst loading flexibility, and cost-effectiveness. In a comparative study conducted by Buhler *et al.*, it was perceived that in PEM water electrolysis, the CCM-MEA exhibited superior kinetics compared to the CCS-MEA. However, despite this advantage, the CCM-MEA demonstrated poorer polarization behaviour and less consistent performance reproducibility than the CCS-MEA, particularly at current densities exceeding 750 mA $cm^{-2}$.[64]

Furthermore, additional benefits of CCM include: (i) enhanced adhesion of the catalytic layer, evidenced by its capability for continuous operation exceeding 20 000 hours; (ii) diminished vulnerability to dimensional alterations when the membrane undergoes drying; (iii) simplified removal of CCMs from stacks to facilitate maintenance purposes; and (iv) reduced levels of contamination arising from gas cross-permeation under high operating pressures. This decrease is ascribed to the presence of catalyst particles situated in the sub-surface section of the membrane, facilitating the re-oxidation of cross-permeating hydrogen by the catalyst.[65]

## 5. CCM preparation process

The preparation process of a CCM for water electrolysis is a crucial factor in determining the efficiency and durability of the

Table 2 Comparative analysis of CCS and CCM strategy

| Criteria | Catalyst coated substrate (CCS) | Catalyst coated membrane (CCM) |
|---|---|---|
| Structure and composition | • The catalyst is directly applied onto a conductive substrate material<br>• Generally, the catalyst layer is composed of noble metals such as Pt, Ir, or $Ru_2O$, which facilitate the electrolysis reactions | • The catalyst is dispersed within or coated onto an ion exchange membrane (AEM or PEM)<br>• The membrane serves both as a support structure and as an ion conductor, facilitating the transport of $H^+/OH^-$ ions between the electrodes |
| Ion transport | • Ion transport relies on the electrolyte solution surrounding the CCS<br>• $H^+$ ions generated at the anode diffuse through the electrolyte to the cathode, while $OH^-$ ions migrate in the opposite direction | • Ion transport occurs directly through the membrane, with $H^+$ ions traveling through the PEM from the anode to the cathode. While $OH^-$ ion migrates through AEM from the cathode to the anode<br>• The direct ion transport pathway leads to faster reaction kinetics and higher efficacy |
| Electrode architecture | • CCS configurations often involve a porous electrode structure, where the catalyst layer is applied onto a high surface area substrate material<br>• This provides ample active sites for electrolysis reactions and allows efficient mass transport of reactants and products | • CCM configuration typically involves a thin catalyst layer coated onto one or both sides of the membrane<br>• This minimizes the diffusion distance for ions and electrons, leading to improved reaction kinetics and reduced ohmic losses compared to the CCS configuration |
| Mechanical integrity | • CCS configuration offers better mechanical stability and durability compared to CCM<br>• The solid substrate provides structural support to the catalyst layer and can withstand mechanical stresses during operation and handling | • CCM configurations are more susceptible to mechanical damage, as the catalyst layer is integrated within the relatively fragile PEM/AEM<br>• Extra care must be taken to prevent delamination or degradation of CCM during operation and maintenance |
| Application flexibility | • CCS configurations are often preferred for large-scale industrial applications, where durability, scalability, and cost-effectiveness are critical factors<br>• The CCS method is more suitable for both alkaline and PEMWE systems | • CCM is well-suited for small to medium-scale electrolysis applications, especially PEMWE systems where high efficiency and rapid response times are desired |

electrolysis system. The CCM preparation process involves several important steps, each requiring careful consideration and optimization to produce high-performing CCMs. The schematic illustration of the CCM preparation process was elucidated in the Fig. 3.

### 5.1. Substrate preparation

**(i) Membrane selection.** The membrane either PEM or AEM serves as the substrate for catalyst coating. Nafion® are most used proton exchange membrane due to their good chemical stability, high proton conductivity, and mechanical strength.

**(ii) Membrane pretreatment.** The membrane surface is often pretreated to increase its hydrophilicity and enhance catalyst adhesion. This can involve treatments like plasma etching, acid treatment, or applying a hydrophilic layer.

### 5.2. Catalyst ink preparation

**(i) Catalyst material selection.** The choice of catalyst materials is critical, with platinum and iridium oxides commonly used for the cathode and anode sides, respectively, in PEM water electrolysers.

**(ii) Ink formulation.** Catalyst particles are dispersed in a solvent along with an ionomer and other additives to form a homogeneous catalyst like. The ionomer acts as a binder and enhances proton conductivity.

### 5.3. Coating process

**(i) Techniques.** Several coating techniques can be used, such as spray coating, screen printing, and decal transfer. Each method has its advantages; for instance, spray coating allows for even distribution of catalyst, while screen printing van produce precise patterns.

**(ii) Layer thickness and uniformity.** Control of the catalysts layer's thickness and uniformity is crucial for optimal performance. This requires precise control over the coating process parameters.

### 5.4. Drying and curing

**(i) Drying.** After coating, the membrane is dried to remove solvents, typically using controlled heating. Drying condition must be carefully managed to prevent membrane damage and ensure uniform catalyst layer adherence.

**(ii) Curing.** The coated membrane may be subjected to a curing process, which can involve further heating under specific conditions to improve the mechanical and chemical bonding layer to the membrane.

### 5.5. Quality control and testing

**(i) Physical inspection.** Visual and microscopic inspections are performed to check for defects or inconsistencies in the catalyst layers.

**(ii) Performance testing.** Electrochemical tests, such as polarization curves and impedance spectroscopy, are conducted to evaluate the CCM's performance characteristics.

## 6. CCM preparation methods

The establishment of suitable preparation methods is crucial for producing stable CCM-MEAs. Various fabrication techniques for CCMs have been developed to meet this demand, including spray coating, decal transfer coating, doctor blade coating, screen-printing, brushing, inkjet printing, layer-by-layer deposition, bar coating, and solvothermal method.[66–68]

### 6.1. Decal method

CCMs can be synthesized using the decal method, initially introduced by Wilson and Gottesfeld.[69,70] This technique offers advantages such as achieving a reduced interfacial resistance between the catalyst layer and the polymeric membrane, creating a thinner catalyst layer with decreased mass transfer resistance, and facilitating better contact among the electrode components.[71] Despite these benefits, the conventional decal process is characterized by its complexity and labour-intensive nature. Moreover, the elevated temperature required for hot-pressing the MEA poses a limitation.[72]

In the traditional decal method, such as in PEMWE, several steps are involved. Firstly, the $H^+$ form Nafion® membrane needs to be converted into the $Na^+$ form membrane through treatment with an appropriate base. Secondly, the catalyst ink is applied onto a Teflon substrate. Subsequently, the catalyst layer is transferred to the membrane *via* hot-pressing at temperatures ranging from 160 to 210 °C.[73] Finally, the catalysed membrane is rehydrated and subjected to ion-exchange to revert to the $H^+$ form by immersion in a hot dilute sulfuric acid solution.

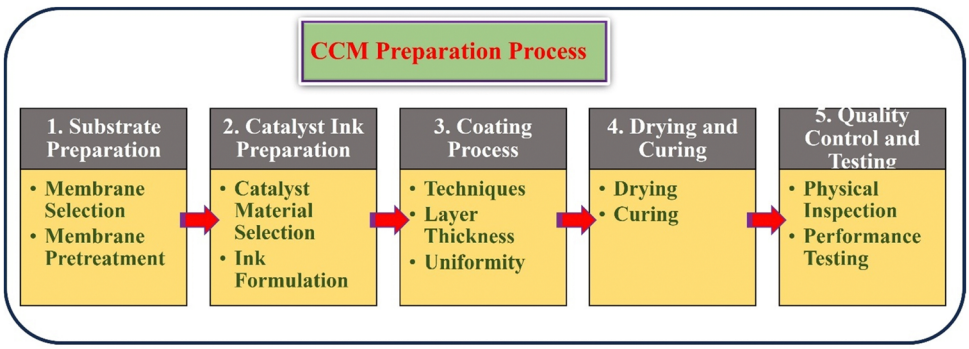


Fig. 3 Schematic sketch of the CCM preparation process.

A recent development involves a low-temperature decal transfer method for MEA fabrication.[70] In this approach, a thin carbon layer is initially deposited onto the Teflon decal substrate, followed by the addition of catalyst and ionomer layers in a manner that sandwiches the catalyst layer between the inner thin carbon and outer ionomer layers. These multi-layer substrates (outer ionomer/catalyst/carbon/substrate) are then hot-pressed on both sides of the $H^+$ form membrane at 140 °C to form the MEA. Despite offering a lower processing temperature, this decal method remains multi-step and necessitates an additional inner carbon layer ad outer ionomer layer.

### 6.2. Screen-printing method

The comprehensive procedure for fabricating CCM-MEA utilizing the direct screen-printing method in PEMWE is detailed below.[74] Initially, the surface of the $H^+$ form Nafion® membrane exhibits significant swelling upon exposure to organic solvents. To ensure smoothness in the resulting screen-printed CCM-MEAs, the initial $H^+$ form Nafion® membrane must undergo conversion to the $K^+$ form. Subsequently, the screen-printing paste is systematically applied to both sides of the resulting $K^+$ form Nafion® membrane using a screen printer. Each application step of the paste onto the $K^+$ form Nafion® membrane is succeeded by thorough drying in an oven. Ultimately, the CCM-MEA with the $K^+$ form membrane undergoes boiling in sulfuric acid to revert the membrane to its $H^+$ form for performance testing.

Typically, the screen-printing paste comprises solubilized Nafion®, catalyst powder, and organic solvents. Occasionally, additives such as plasticizers or silicas may be incorporated into the screen-printing paste to confer specialized properties upon the fabricated CCM-MEAs. The formulation of the screen-printing paste, particularly the judicious selection of solvents, serves as a critical determinant for producing high-quality CCM-MEAs. However, no ample literatures have thus far been reported in the domain of water electrolysis systems employing the screen-printing procedure for fabricating CCM-based MEAs.

### 6.3. Spray coating method

One of the most established and frequently used methods in CCM-MEA fabrication is spray coating. In a typical procedure for preparing the catalyst in layers using the spray method, a blend of commercial Pt/C or $IrO_2$ electrocatalyst, 5 wt% Nafion® solution, isopropanol, and deionized water is meticulously mixed in optimized weight proportions and stirred supersonically for 1 h.[75] An air-driven spray gun is employed to apply controlled amounts of anode and cathode inks onto the decal substrate. The coated PTFE sheet is carefully weighed after drying at 100 °C, then hot-pressed on each side of a pre-treated Nafion® membrane at approximately 135 °C under a pressure of about 4 MPa. Subsequently, the PTFE sheet is removed, and another weighing is performed to determine the final amount of catalyst transferred to the membrane.

### 6.4. Brushing method

In the fabrication of CCM-MEA through the brushing procedure for catalyst ink preparation, the typical protocol involves several steps. Initially, the catalyst is commonly combined with glycerol, 5 wt% Nafion® ionomer, and tetrabutylammonium hydroxide (TBAOH) in 1 mL methanol, followed by overnight stirring to ensure thorough dispersion. Subsequently, this dispersion is brush-painted onto a decal, Teflon-coated fibre glass surface, and then subjected to heating and drying at 140 °C for 30 min. The resulting coated PTFE sheet undergoes careful weighing before being hot-pressed on both sides of a pre-treated Nafion® membrane at 210 °C for 5 min under a pressure of 454 kg $cm^{-2}$. Finally, the PTFE sheet is removed, and a subsequent weighing is conducted to determine the final amount of catalyst transferred onto the membrane.[76]

In summary, while various methods exist for fabricating MEAs using catalyst coated membranes, the most used approaches are spray coating and the decal method. This preference stems from their ease of operation and efficient time management characteristics. Spray coating and the decal method offer researchers straightforward procedures with manageable time requirements, making them attractive choices for the fabrication of MEAs with catalyst coated membranes in numerous research and industrial settings.

## 7. Physical and structural analysis of CCM

CCMs play a pivotal role in the performance of MEAs by enhancing the uniformity of catalyst layers on membranes, which significantly reduce contact resistance. Zhang *et al.* explored the microstructure of CCMs fabricated using a direct spray deposition technique, as observed under scanning electron microscopy (SEM).[77] The SEM image in Fig. 4(a) depicts the anode's surface, showcasing the $Ir_{0.6}Mn_{0.4}O_x$ catalyst particles evenly distributed and encapsulated by Nafion ionomers. The cathode features PtNi alloy particles, supported by a carbon carrier and Nafion ionomers (Fig. 4(b)). Notably, the cathode catalyst particles are finer than those at the anode, and evenly distributed throughout the layer, indicative of effective coating and blending of the $Pt_1Ni_3$/C with Nafion ionomers. Additionally, Fig. 4(e) represents the SEM image of the CCMs cross-section. Despite deformation caused by compression during sample preparation, the catalyst layers maintain a consistent, albeit thinner, thickness compared to the membrane, highlighting the structural integrity of the CCM under mechanical stress Fig. 4(c) and (d) represents the elemental mapping images of $Ir_{0.6}Mn_{0.4}O_x$ and $Pt_1Ni_3$/C, respectively.

## 8. Electrochemical performance evolution of CCM

The electrochemical characterization of CCM in the context of MEAs is a key aspect of assessing their performance in electrochemical devices like electrolyzers and fuel cell.

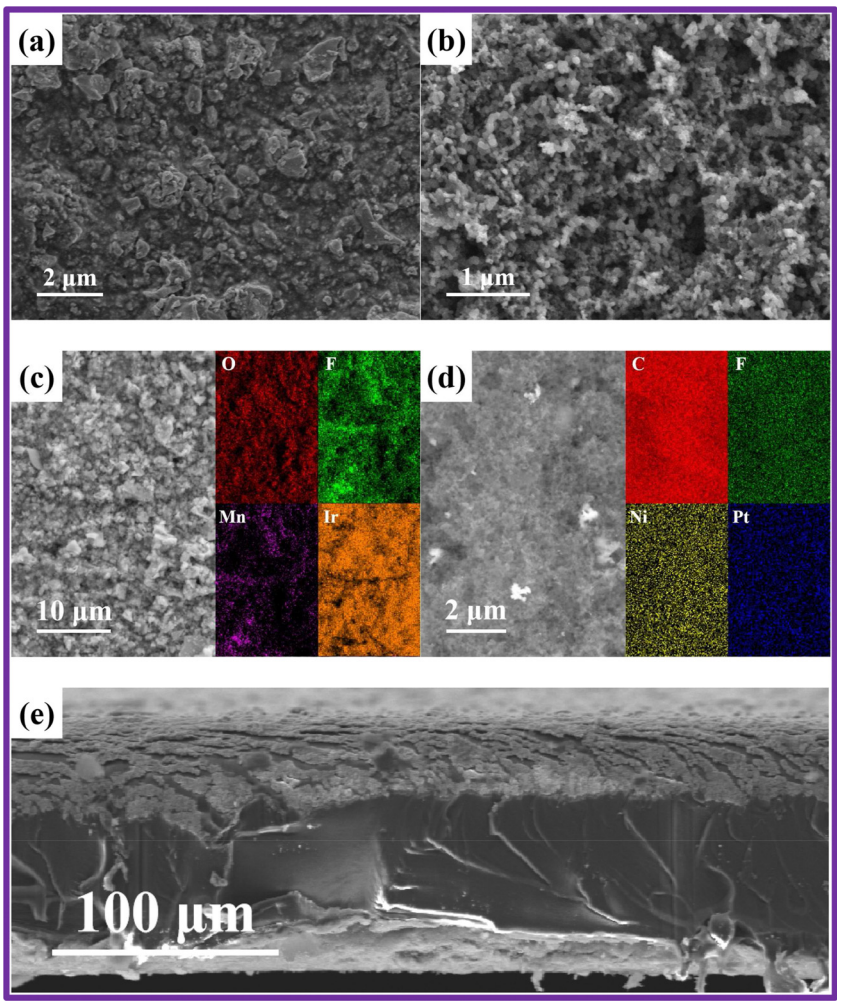


Fig. 4 Microstructural analysis of CCM surface and cross-section. (a) SEM depiction of the anode catalyst layer; (b) SEM portrayal of the cathode catalyst layer; (c) elemental distribution in the anode catalyst layer; (d) elemental distribution in the cathode catalyst layer; (e) SEM visualization of the cross-sectional view. Reproduced with the permission from ref. 77. Copyright 2023, Elsevier.

### 8.1. Polarization curve

The efficiency of water electrolysers is greatly influenced by internal factors such as the catalyst and MEA configuration, as well as eternal conditions such as temperature, liquid flow rate, and pressure. Consequently, it is crucial for water electrolysers to be meticulously assembled and tested under stable conditions to ensure consistent performance. Additionally, proper preconditioning of the cell is essential before conducting performance evaluations. For PEMWE/AEMWE, the galvanostatic method, known as chronopotentiometry (CP) is generally more advantageous for precise performance assessments compared to cyclic voltammetry (CV) and linear sweep voltammetry (LSV), which are typically used to evaluate catalyst performance in three-electrode systems under more favourable diffusion and transfer conditions. Specifically, at high current densities, CV measurements taken at rapid scan rates may be hampered by slow mass transfer processes. This rapid voltage change fails to maintain a stable reaction system, leading to inaccurate and less reproducible current–voltage responses. In contrast, CP monitors the potential over time at a consistent current, allowing the system to stabilize the potential adequately. By conducting multiple CP tests, one can obtain a reliable polarization curve of the cell. It should be noted that while CV can also provide accurate performance data if the sweep rate is sufficiently slow (0.5 mV $s^{-1}$), recording a single curve could take several hours.

Fig. 5 illustrates the standard polarization curve for an AEMWE, depicted by a black dotted line. This curve was obtained in a 2-electrode system using a galvanostatic approach, where variable current densities ranging from 0.01 to 5 A $cm^{-2}$ were applied in steps, each maintained for 0.5 to 2 minutes to stabilize the potential response.[78] Additionally, Fig. 3 includes a breakdown of the predicted cell voltage components: the reversible cell voltage (also termed thermodynamic potential, measured at 1.229 V under standard conditions), ohmic overpotential, and activation overpotentials at the anode and cathode. The overpotential is indicative of the combined electrical and ionic resistances of the membrane, electrode, bipolar plates, current collectors, and connecting wires. Activation overpotentials are primarily influenced by the catalyst's effectiveness and the MEA

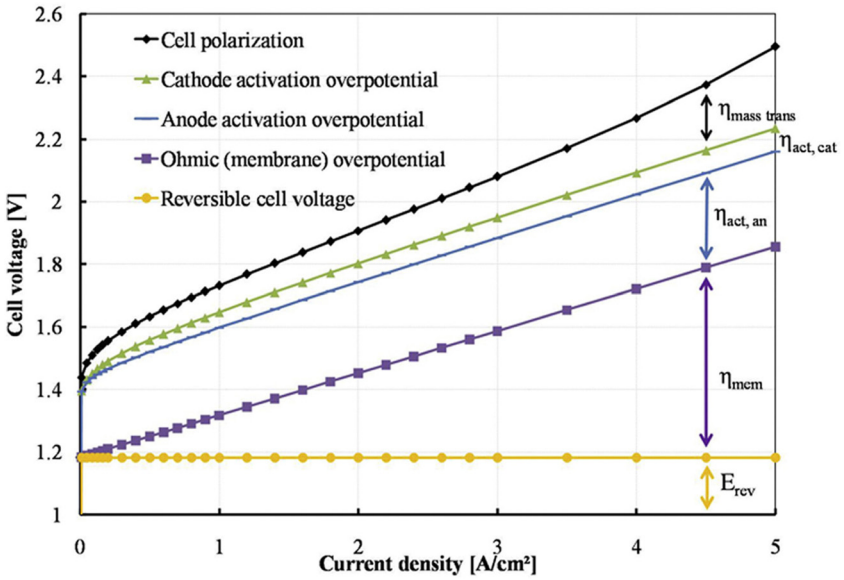


Fig. 5 Potential distribution of polarization curve. Reproduced with the permission from ref. 78. Copyright 2017, Elsevier.

dynamics. The polarization curve is segmented into three distinct regions based on the current density:[79–81] (i) below 0.2 A $cm^{-2}$ where activation losses at the anode and cathode are prominent; (ii) between 0.2 and 4 A $cm^{-2}$ here resistance losses escalate with increasing current density; and (iii) above 4 A $cm^{-2}$ where significant mass-transport losses are observed. These observations provide crucial insights into the AEMWE's performance, emphasizing the importance of tuning both internal and external factors across different operational regions.

### 8.2. Electrochemical impedance spectroscopy

EIS is a critical technique for assessing the impedance of water electrolyser systems across various frequencies. This method is instrumental in detecting and quantifying different types of losses that affect the cell performance, including ohmic, charge transfer, and mass transfer losses. In EIS, the frequency response of the impedance is measured by introducing a small amplitude alternating current or voltage in either galvanostatic or potentiostatic mode. The data obtained are commonly represented in Nyquist plots, which are then analysed to derive an equivalent electrical circuit (EEC) model.[82] This model visually represents the comparative scale of the various resistances within the cell, providing insights into the underlying physical processes of the water electrolyser, thereby guiding the selection of the most suitable EEC model for accurate interpretation and analysis.[83,84]

Fig. 6(a) represents the Nyquist plot and ECC for an AEMWE, revealing various resistance components. The ECC consists of an ohmic resistance ($R_0$) in series with an inductor ($L$), attributed to cables and wires, and three parallel circuits each combining a resistor with a constant phase element (CPE).[85] The CPE represents the double layer capacitance ($C_{dl}$) of the HER and OER. $R_0$ captures the internal ohmic resistance from the membrane, electrode, gas diffusion layer, bipolar plates, and contact points.[86] The middle-frequency semi-circle of the Nyquist plot helps determine the charge transfer resistances $R_1$ for HER and $R_2$ for OER, where OER's complex four-electron process results in a higher resistance ($R_2 > R_1$).[87] $R_3$, visible at the plot's low frequency, denotes the mass transfer resistance, significantly influenced by the efficiency of water/gas flux management in the GDL structure.[88] Inefficient water supply and delayed gas removal elevate mass transfer resistance, contributing to higher contact resistance and blockage of active sites, adversely affecting overall cell performance. Thus, EIS analysis provides deep insights into the electrochemical kinetics of water electrolyser, aiding in understanding the reaction mechanisms and advancing the technology.

## 9. Fabrication of MEA by CCM method in AEMWEs

Park *et al.* focuses on enhancing efficiency and durability of AEMWE through innovative CCMs (introduces macroporous catalyst layer design).[89] Utilising iridium oxide and 40 wt% Pt/C was employed as the anode and cathode catalysts, respectively. The constructed CCM-MEA demonstrated superior performance (1.9 V at 2760 mA $cm^{-2}$) and durability at 70 °C, attributed to improve mass transport and reduced resistances. The macroporous CL design significantly outperforms conventional plain catalyst layers by improving catalyst utilization, reducing ohmic and charge-transfer resistances, and achieving higher current densities. Furthermore, the macroporous structure provides better durability and mass transport, which are crucial for operational stability. While the design offers reduced catalyst loading and potentially lower costs, its complexity and scalability pose challenges.

Jaromír Hnat *et al.* reported a CCM leveraging non-precious metal catalysts, $NiCo_2O_4$ for the anode, and $NiFe_2O_4$ for the

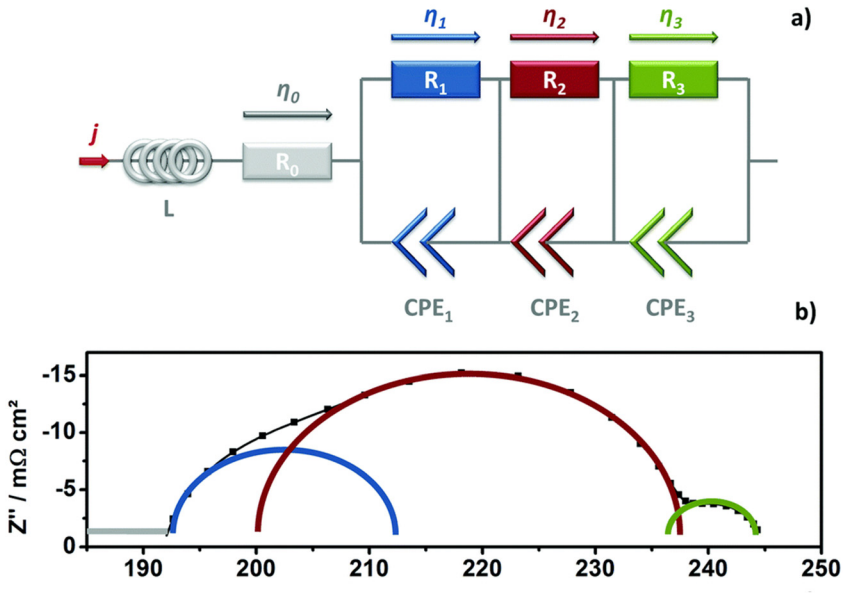


Fig. 6 (a) Diagram of the equivalent circuit used for EIS analysis; (b) illustration of a Nyquist plot displaying analyzed arcs (time constants). Reproduced with the permission from ref. 82. Copyright 2017, RSC.

cathode, with an anion-selective polymer binder, aiming at reducing catalyst loading while maintaining high performance for AEMWEs.[90] Utilizing a hot plate spraying technique for electrode deposition on a polystyrene-*block*-poly(ethylene-ran-butylene)-*block*-polystyrene (PSEBS) membrane functionalized with diazabicyclo [2.2.2] octane (DABCO) groups, this innovative approach showed promising electrochemical properties under alkaline AEMWE conditions. The SEM analysis confirmed good contact between the catalyst layers and the membrane, both before (Fig. 7(a) and (c)) and after the electrolysis experiment (Fig. 7(b) and (d)), highlighting the catalyst layers' mechanical stability without delamination. Remarkably, even under harsh anodic oxygen evolution conditions, the ionomer binder maintained necessary mechanical characteristics, preventing catalyst removal or delamination from the surface of the membrane. Performance evaluation between CCM-MEAs and CCS-MEAs demonstrated slightly superior results for CCM-MEAs with 10 mg $cm^{-2}$ catalyst load due to better catalyst utilization (Fig. 7(e)). Surprisingly, reducing the catalyst load to 2.5 mg $cm^{-2}$ had an insignificant impact on performance, particularly at lower current loads, signifying efficient catalyst utilization at reduced loadings. The polarization resistance ($R_p$; anode) values indicated that the CCM-MEA (Fig. 7(f)) with 2.5 mg $cm^{-2}$ catalyst load exhibited the lowest cell resistivity of 0.030 Ω $cm^2$, attributed to the low resistivity of the catalyst layer. The Nyquist and Bode plots further supported these findings and it was shown in Fig. 7(d) and (e). A comparison between the CCM-MEA with 10 mg $cm^{-2}$ catalyst load and the CCS-MEA revealed lower $R_s$ values for the CCS-MEA (0.043 and 0.038 Ω $cm^2$ respectively). The study

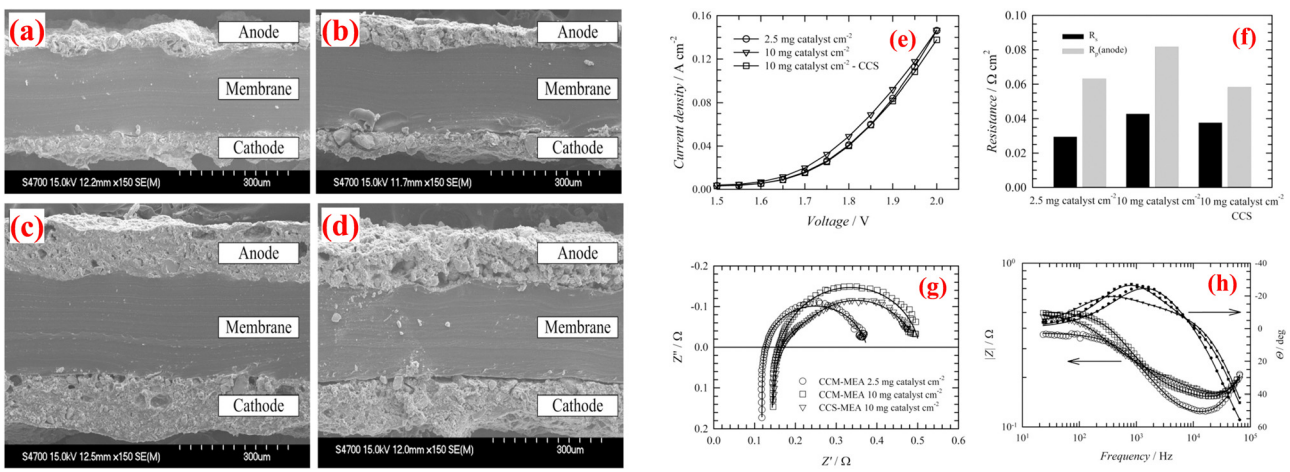


Fig. 7 Cross-sectional SEM pictures of the CCMs before (a), (c) and after (b), (d) AEMWE performance; (e) polarization curves of AEMWE with various membranes; (f) values of $R_s$ and $R_p$; (g) EIS; and (h) Bode plot. Reproduced with the permission from ref. 90. Copyright 2019, Elsevier.

underscores the potential of CCM technology in AEMWE using non-precious metal catalysts, offering a cost-effective and efficient approach to hydrogen production, while acknowledging the necessity for the further optimization of catalyst layer composition and preparation methods to enhance performance and durability. The demonstrated stability and compatibility of the CCM with the membrane represent a significant advancement in WE technology. Electrolysis experiments conducted at 45 °C in 10 wt% KOH solution and a flow rate of 5 mL $min^{-1}$, with load curves recorded in a voltage range from 1.5 to 2.0 V, exhibited stable operation at a current load of 0.25 A $cm^{-2}$.

Gatto *et al.* utilized the FUMASEP® FAA3-50 anion-exchange membrane focusing on optimizing performance through several operational parameters (effects of catalyst loading, electrolyte concentration, and operational temperature).[91] It employs a CCM approach with commercial $IrO_2$ as the anode catalyst and 40% Pt/C as the cathode catalysts to enhance reaction kinetics at elevated temperatures and improve overall efficiency. Key findings include the necessity of diluted KOH solution for maintaining conductivity and performance, indicating a trade-off between operational efficiency and system complexity. Future direction suggests that exploring cost-effective alternatives to $IrO_2$ to reduce expenses while maintaining or improving electrolyser performance, emphasizing the balance between technological efficiency and economic viability in hydrogen production.

Lou *et al.* studied the advancements in AEMWE focusing on the innovative use of 'accessional ionomer coatings' to enhance catalyst architectures for high performance.[92] It explores the integration of ionomer interlayers within membrane electrode assemblies (MEAs) which notably improve cell performance due to increased electrochemical surface area (ECSA). The use of ionomer interlayers leads to reduced overpotential and degradation over 150 hours of operation, highlighting durability improvements. Specifically, the study demonstrates how ionomer modified CCS and CCM configurations enhance the operational stability and efficiency of the electrolyser systems. A hybrid CCS–CCM configuration is introduced, utilizing cost-effective NiFe catalysts which shows comparable catalytic activity and increased durability compared to more expensive noble metal catalysts like iridium. These findings emphasize that thorough architectural and structural development of the ionomer and catalyst layers, AEMWE systems can achieve enhanced performance and longevity, paving the way for more sustainable and economically feasible hydrogen production.

Plevova *et al.* examines the optimization of MEA for alkaline water electrolysis using CCMs, employing chloromethylated PSEBS polymers functionalized with DABCO and non-precious metal catalysts ($NiCo_2O_4$ and $NiFe_2O_4$) for enhanced durability and cost-effectiveness. It identifies an optimal catalyst-to-binder ratio that ensures stable performance over 140 hours, highlighting a reduced need for high-concentration KOH solutions due to effective ionic interaction provided by the ionomer.[93] The findings advocate further research into cost-effective materials to improve the economic viability and operational sustainability of water electrolysis technologies.

Chen *et al.* utilizes hexamethyl-*p*-terphenyl poly(benzimidazolium) [HMT-PMBI] as the membrane materials, which shows notable robustness and stability in AEMWE.[94] AEMWE application in 1 M KOH at 60 °C exhibited negligible degradation over 100 hours at a current density of 240 mA $cm^{-2}$ and a cell voltage of 1.74 V, underscoring its durability and stability. The performance and durability of the cell is significantly influenced by the concentration of the KOH electrolyte. Lower concentration or pure water led to decreased voltage stability, which is attributed to increased swelling of the ionomer within the catalyst layer. The main advantage of using HMT-PMBI based CCMs is their enhanced stability and robustness under alkaline conditions, crucial for long-term operational stability. However, a significant disadvantage is the complex management of ionomer and membrane swelling, which can adversely affect the cell's performance and longevity if not properly controlled. Furthermore, the Chet *et al.* suggested that future research should focus on developing ionomer materials that combine reduced volumetric swelling with high chemical stability to extend the operational life of AEMWEs, especially in challenging conditions like pure water electrolysis.

Lazaro *et al.* investigated the $NiFe_2O_4$ hierarchical nanoparticles synthesized *via* hydrothermal method with glucose and urea as precursors, serving as an efficient electrocatalyst for an AEMWE using a Fumasep® FAA3-50 membrane.[95] This configuration achieves a notable current density of 2.7 A $cm^{-2}$ at 2.2 V and 60 °C, surpassing traditional $IrO_2$ catalysts by over 25%. The catalysts enhanced performance and promising 72-hour durability test results highlights its potential for sustainable and cost-effective hydrogen production, presenting a significant advancement in employing noon-precious metal catalysts for water electrolysis.

Kong *et al.* developed a new method for fabricating a modified CCM (m-CCM) for AEMWEs that does not use ionomers.[96] Generally, ionomers are typically used as physical binders for catalyst layers (CLs), but they can hinder the exposure of the catalyst and the transport of gaseous products. The m-CCM method permits for the direct growth of the CLs between the AEM and the GDL, without using any ionomers. This methodology enhances the interconnection between layers, maximizes catalyst utilization, and diminishes resistance at the cell interface. Assembly of the AEMWE involves circulating a reducing agent (1 M $NaBH_4$) and metal precursor solution (Ni : Fe in a 3 : 1 ratio) through it. This triggers a chemical reduction reaction, enabling the $BH_4^-$ ions to transfer *via* the AEM to the anodic compartment, where they reduce $Ni^{2+}$ and $Fe^{3+}$ ions, forming the catalyst layer directly on the AEM surface. This technique ensures close contact between the AEM and CL, leading to enhanced electrochemical performance of the AEMWE. A schematic sketch of the m-CCM method was exhibited in Fig. 8(a). Field-emission scanning electron microscopy (FE-SEM) was conducted to investigate the surface topography of the CLs grown directly *via* the ionomer-free m-CCM method. In Fig. 8(b), the catalyst layer displays vertically interlaced nanosheet structures grown on the surface of the AEM (Sustainion X37-50). The cross-section view of FE-SEM pictures

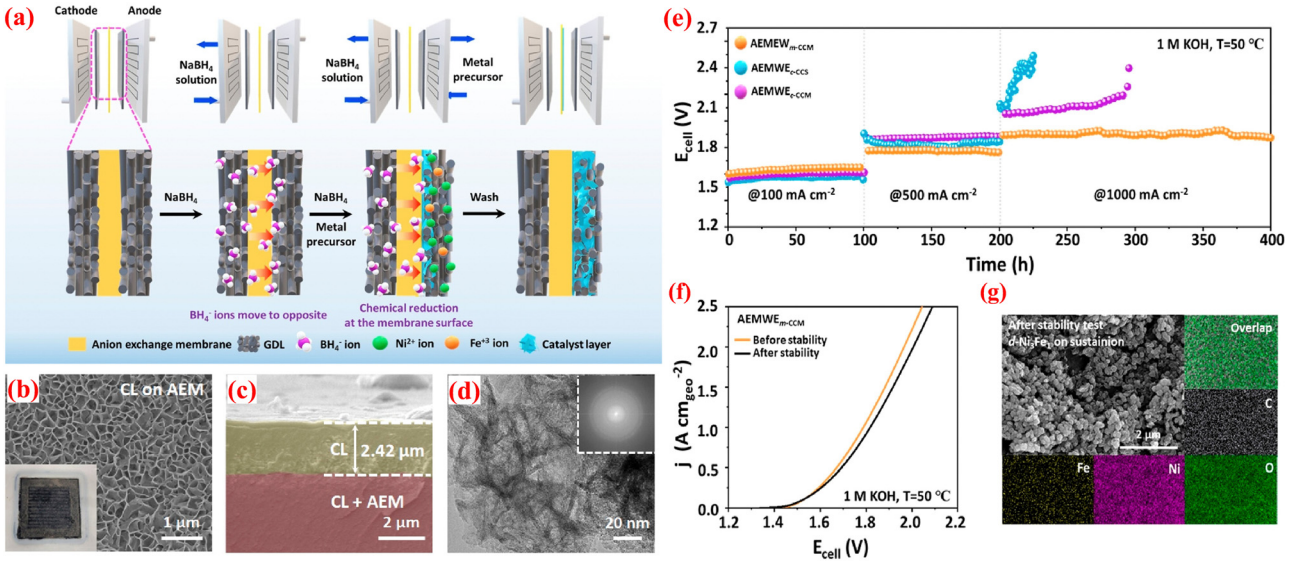


Fig. 8 (a) Schematic view of *in situ* ionomer-free m-CCM method; FE-SEM images of d-$Ni_3Fe_1$ CLs (b) arial view; (c) cross-section view; (d) HR-TEM image of d-$Ni_3Fe_1$ CL (inset: FFT pattern); (e) long-term durability study of AEMWEs at constant current densities; (f) polarization curves of AEMWEs using m-CCM with Sustainion X37-50 before and after long-term stability test; and (g) SEM an EDS mapping studies of d-$Ni_3Fe_1$ CLs on Sustainion X37-50 after the stability test. Reproduced with the permission from ref. 96. Copyright 2013, ACS.

reveals that the CL, approximately 2.5 µm thick, maintains unvarying and close contact with the anion exchange membrane (Fig. 8(c)). HR-TEM and energy-dispersive X-ray spectroscopy (EDS) analyses were performed to further examine the morphologies of the synthesized CLs on the AEM, (Fig. 8(d)). They depict interlaced nanosheet morphologies consistent with the SEM image. The corresponding fast-Fourier-transformed (FFT) image (inset in Fig. 8(d)) indicates an amorphous structure. To access the long-term durability of the AEMWEs, nonstop electrolysis was conducted at constant current densities of 100, 500, and 1000 mA $cm^{-2}$ for 400 h. As depicted in Fig. 8(e), AEMWEm-CCM demonstrates steady electrolysis performance at all applied current densities compared to conventionally fabricated AEMWEs. Particularly, AEMWEm-CCM exhibited minimal activity degradation for 200 h at an industrially relevant current density of 1 A $cm^{-2}$, attributed to optimal contact at the AEM–CLs interface enhancing CLs adhesion and a vertically aligned layered nanosheet morphology facilitating bubble management at high current densities. Additionally, aside from continuous electrolysis, AEMWEm-CCM instantaneously responds to applied current density, showcasing greater mass transport characteristics and mechanical robustness of m-CCM derived MEAs. Fig. 8(f) indicates a nominal activity degradation rate of 0.07 mV $h^{-1}$ at 1 A $cm^{-2}$ after the long-term durability test. The structural stability of d-$Ni_3Fe_1$ was further confirmed by SEM after 400 h of nonstop electrolysis (Fig. 8(g)). Although d-$Ni_3Fe_1$ is agglomerated, it still retains nanosheet morphology and uniform elemental distribution of Ni, Fe, O, and C. Furthermore, the *in situ* ionomer-free m-CCM technique has been demonstrated to significantly enhance the efficacy and stability of AEMWEs by optimizing the membrane–electrode interface. This method overcomes the constraints associated with anion exchange ionomer (AEI), such as decreased catalyst exposure and hindered mass transport, and presents a promising avenue for the creation of dependable and efficient AEMWEs for commercial hydrogen production.

Koch *et al.* presented a method for producing CCMs for AEMWE by direct deposition of the catalyst in a bar coating process.[97] The process steps for direct coating the CCM using bar coating are illustrated in Fig. 9. To summarize, in the fabrication of directly coated CCMs, a membrane was affixed to a clean glass surface and shielded with a polytetrafluoroethylene (PTFE) patch along the upper edge. A drop of anode ink was meticulously positioned on the patch (Fig. 9-(1)) and uniformly spread across the membrane (Fig. 9-(2)) using a bar coater. After drying, half of the CCM was covered with a blue adhesive foil, while a grey PTFE foil safeguarded the electrode layer (Fig. 9-(3)). The backing sheet (petrol) was peeled off and the half-CCM was affixed to the glass surface with the uncoated side facing upward. Another drop of cathode ink was meticulously placed on a separate PTFE patch (Fig. 9-(4)) and evenly distributed over the membrane using the bar coater (Fig. 9-(5)). Throughout the drying process, the combination of PTFE foil and adhesive foil creates slight tension on the CCM, preventing wrinkling in the active area (Fig. 9-(6)). The performance of the directly coated CCMs is compared to spray-coated ones, and it is found that the direct coating method yields results that are either equal to or better than spray coating, particularly at higher current densities with a significant reduction in mass transport limitations. They have used Aemion+ membranes and catalysts such as $IrO_2$ and Pt/C, intending to achieve high efficiency and durability.

Kiessling *et al.* explored the hydroxide exchange membrane water electrolysis (HEMWE), utilizing a Tokuyama A201 membrane, catalyst loadings were set at 2 mg $cm^{-2}$ for $IrO_2$

and 1 mg $cm^{-2}$ for 50 wt% Pt/C, with the CCMs prepared *via* ultrasonic spray coating.[98] Key findings highlight that catholyte composition crucially affects membrane hydration and operational efficiency, where carbonate ions in the catholyte adversely impact cell performance, and increased cation/$OH^-$ ratios lead to higher cell potentials. These insights are pivotal for optimizing electrolyte management in water electrolysis systems to enhance the efficiency and durability of green hydrogen production.

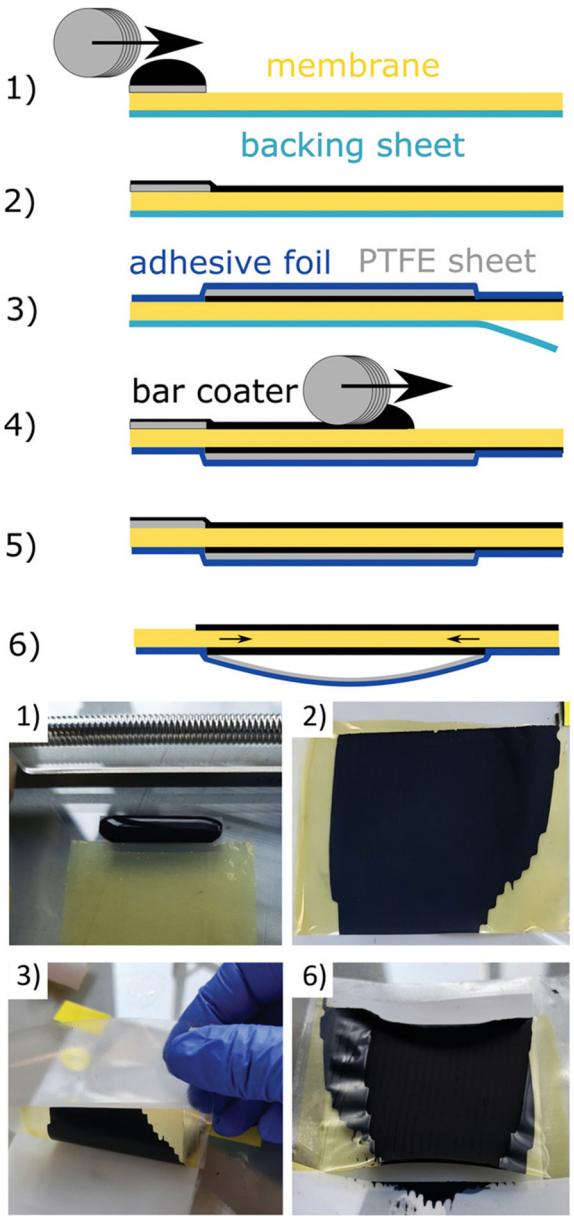


Fig. 9 Fabrication steps of a directly coated CCM with bar coating method. (1), (2) use of the first catalyst layer; (3) use of a protective PTFE layer (grey) with an overlapping adhesive film (blue); (4), (5) use of the second catalyst layer Mayer-rod; (6) the PTFE layer creates gentle tension during drying/shrinking of the CL which protects the CCM from wrinkling. Reproduced with the permission from ref. 97. Copyright 2023, John Wiley and Sons.

Ozawa *et al.* studied a novel approach "*in situ* ionomer-free CCMs for AEMWE" It introduces a unique method for preparing ionomer-free CCMs, focusing on the direct growth of CLs on the anion exchange membrane (QBM-2.7).[99] Moreover, when paired with Ni0.8Co0.2O and Pt/C catalysts, the QBM-2.7 membrane achieved notable electrolysis performance, with an onset voltage of 1.44 V and a cell voltage of 1.62 V at 1.0 A $cm^2$. This approach effectively reduces interfacial resistance and enhances catalyst utilization, leading to superior performance compared to traditional methods that us ionomers. Furthermore, the study showcases the use of platinum group metal-free (PGM-free) catalysts in this new configuration, which not only lowers the material costs but also maintains high efficiency and durability under prolonged operation conditions. This research could significantly impact the scalability and commercial viability of hydrogen production technologies, presenting a promising advancement towards more sustainable energy solutions.

Qiu *et al.* studied the development of hydrogen bond-dominated polybenzimidazole (PBI) semi-interpenetrating network membranes for AEMWEs.[100] The membranes were created using a solution casting method with varying concentrations of TPPR. The cross-linked C-PBI/TPPR-sIPN membranes were produced by treating the PBI/TPPR membranes with different concentrations of HCHO and HCl solutions. The schematic representation of the preparation of PBI/TPPR and C-PBI/TPPR membrane is depicted in Fig. 10(a). To evaluate the practical application of the C-PBI/TPPR-16F membrane in AEMWE, researchers constructed an electrolytic system using the MEA, as depicted in Fig. 10(b). Fig. 10(c) illustrates the polarization curves of different anode catalysts performed in 1 M KOH at ambient temperature employing the same commercial FAA-3-50 membrane. Remarkably, the performance of the NiFe catalyst surpassed that of $IrO_2$. This superiority can be attributed to the layered structure of the mesoporous NiFe catalyst on the macroporous nickel foam (NF) framework, offering numerous active sites exposed to the electrolyte. Additionally, Fig. 10(d) presents the polarization curves of various membranes operated in a 1 M KOH solution at room temperature. Notably, the overpotential of the MEA with the C-PBI/TPPR-12F membrane was 0.2 V lowers than that of the commercial FAA-3-50 membrane. This reduced overpotential suggests that the MEA utilizing the C-PBI/TPPR-12F membrane has a more favourable impact on AEMWE systems. Furthermore, at a cell voltage of 2.0 V, the MEA employing the PBI/TPPR-12F membrane achieved a significantly higher current density of 713 mA $cm^{-2}$ compared to the commercial FAA-3-50 (243 mA $cm^{-2}$) and pristine PBI (369 mA $cm^{-2}$) membranes. The performance of water electrolysis demonstrated a positive correlation with temperature, showing gradual improvement as temperature increased. Specifically, the current density increased gradually from 713 mA $cm^{-2}$ at 25 °C to 890 mA $cm^{-2}$ at 60 °C at 2.0 V (Fig. 10(e)). Moreover, the C-PBI/TPPR-12F membrane achieved a current density of 1 A $cm^{-2}$ at a voltage of 2.05 V. The durability of MEAs using both the C-PBI/TPPR-12F and commercial FAA-3-50 membranes in 1 M KOH was assessed

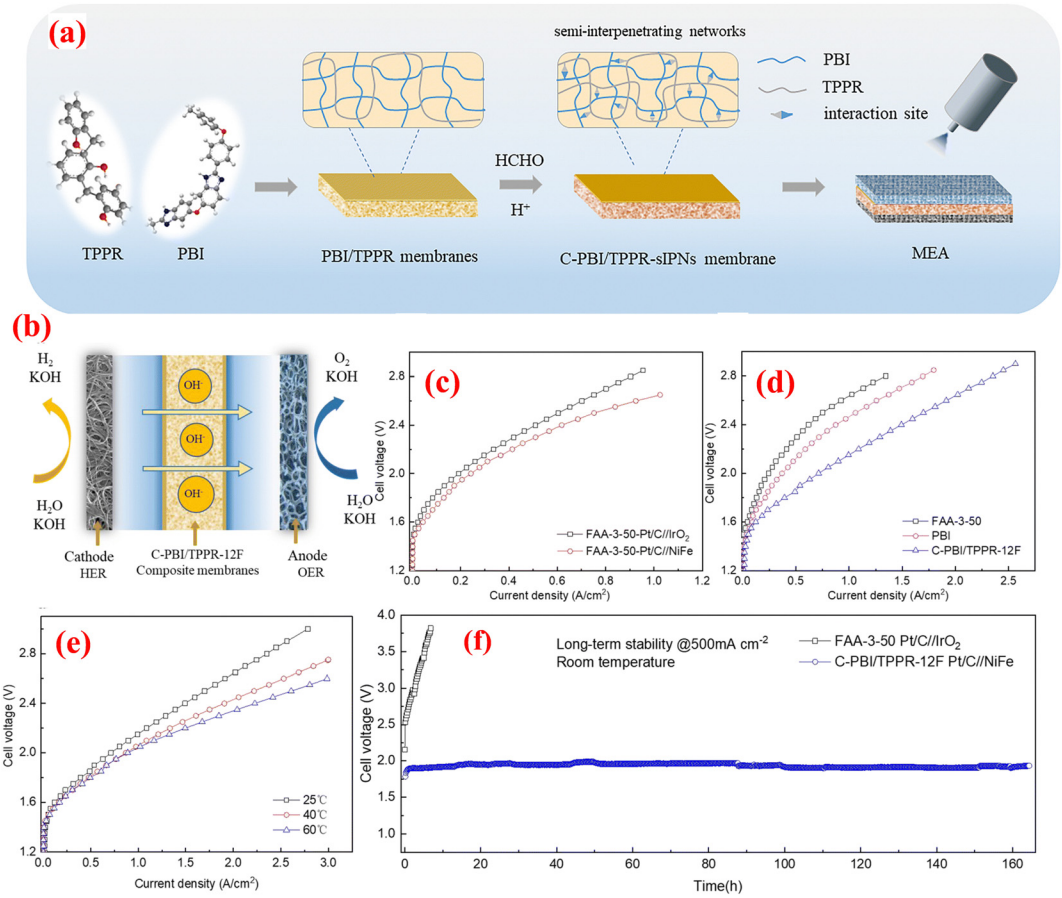


Fig. 10 (a) preparation of PBI/TPPR and C-PBI/TPPR membrane; (b) constructed AEMWE system; (c) polarization curves of different anode catalysts in 1 M KOH at RT; (d) polarization curves of different membranes in 1 M KOH at RT; (e) polarization curves of C-PBI/TPPR-12F membrane at different temperatures; and (f) long-term stability test of commercial FAA-350 and C-PBI/TPPR-12F membranes at 500 mA $cm^{-2}$. Reproduced with the permission from ref. 100. Copyright 2023, RSC.

under a constant current density of 500 mA $cm^{-2}$ at ambient and elevated temperatures. As depicted in Fig. 10(f), the voltage of the CPBI/TPPR-12F membrane with precious group metal-free (PGM-free) anode catalysts largely remained below 2.0 V for over 160 hours. In contrast, the commercial FAA-3-50 membranes with PGM catalysts exhibited comparatively lower electrolytic stability, with the electrolytic voltage rapidly increasing within a short duration. The authors concluded that this membrane type offers numerous advantages for alkaline water electrolysis, including increased hydroxide ion conductivity, improved mechanical and thermal stability, efficient ion transport mechanisms, and reduced overpotential. However, the synthesis of this membrane can be complex, and precise control over the cross-linking process is necessary to achieve optimal performance and durability. The research presented here demonstrates the significant advancements made with the development of PBI/TPPR-sIPN membranes and showcases their potential to address current limitations in membrane performance and durability.

Koch *et al.* studied the AEMWE and examined the impact of AEI concentration on the performance and durability of CCMs in AEMWEs through the use of Aemion+™ reinforced membranes and varying AEI content.[101] They have investigated the anode material comprised of IrOx catalyst particles while adjusting the ionomer content to evaluate its impact on the electrochemical performance of the system. However, the cathode material was not specifically addressed; rather, the focus was on optimizing the anode catalyst layer. Durability examinations were carried out at a current density of 1 A $cm^{-2}$, and it was observed that cells containing 7 wt% and 10 wt% ionomers exhibited promising stability, with degradation rates below 10 mV $h^{-1}$. The electrolyser was operated in a low molarity KOH solution, showcasing the material's resilience in various alkaline conditions. The study demonstrated several advantages, including improved catalyst utilization with reduced IrOx loading in comparison to prior research, promoting efficient resource management. The optimized content of AEI also contributed to enhanced membrane mechanical properties and operational stability. However, it was observed that maintaining consistent catalyst distribution with higher ionomer contents may result in inconsistencies in performance due to increased electrical resistance and diminished gas diffusion capabilities. The outcomes of the study emphasize the necessity of incorporating AEI content in the development of effective CCMs for AEMWEs. By adjusting the AEI content, there exists a

suitable equilibrium between the anode's electrical conductivity, ion exchange capacity (IEC), and overall electrolyser performance. The optimized AEI content not only resulted in an enhancement of water-splitting efficiency but also bolstered the durability of the CCM, making it a prospective solution for sustainable hydrogen production.

Recently, Angela Caprì *et al.* demonstrated nickel ferrite-derived OER catalysts for AEMWE systems.[102] In brief, the nickel ferrite was deposited by spray coating technique onto a Fumasep® FAA3-50 AEM to realize a CCM and analysed in a single cell (5 $cm^2$) set-up in the so-called zero-gap configuration. At 60 °C, the maximum performance of 2.2 V was achieved at a current density of 3 A $cm^{-2}$, which surpasses the commercial catalysts of NiO and $IrO_2$. Furthermore, the prepared CCM-MEA exhibited good stability and it is evident from the chronoamperometry test of 120 h without any changes in the obtained results.

Table 3 summarizes the recent CCM-MEAs reported for AEMWEs. In summary, CCMs have evolved significantly, enabling the advancement of AEM water electrolysers for hydrogen production. While there are challenges such as cost and durability, ongoing research and development efforts aim to further enhance their performance and make them a key player in the transition to a hydrogen-based economy.

## 10. Fabrication of MEA by CCM method in PEMWEs

Hrbek *et al.* presents an innovative approach to manufacturing low-loading catalyst-coated membranes for water electrolysis using a completely dry process. This method involves simultaneous plasma etching of the PEM and deposition of a cerium oxide layer, creating a pronounced fibre-like structure on the membrane surface which can support catalysts without the need for additional nanoparticles.[103] The study highlights the efficiency of this method in reducing noble metal loading (Pt and Ir) to just 220 mg $cm^{-2}$ while achieving high electrolyser performance, emphasizing the potential for scaling up this technology for industrial applications. The research underscores the importance of controlling the working pressure during the sputter-etching process to tune the level of porosity and achieve optimal performance, offering a significant advancement in the fabrication of CCMs for sustainable hydrogen production.

Xie *et al.* conducted a study focusing on optimizing CCMs and performing a comparative analysis between decal transfer and direct spray deposition methods for CCM fabrication. This investigation highlights the significant impact of Nafion® ionomer content within the anode catalyst layer on the overall performance of PEMECs.[104] Fig. 11(a) and (b) represents the SEM images (aerial view) of the $IrO_2$ catalyst layer at the anode prepared using the Decal method. The images reveal a uniform distribution of $IrO_2$ nanoparticles within the CL, coated effectively with Nafion® binder material. Some larger Nafion® particles are also observed, likely resulting from excess Nafion® binder melting during the hot-pressing process. In contrast, Fig. 11(c) and (d) shows the Pt black catalyst layer at the cathode, predominantly consisting of agglomerated Pt particles with a Nafion® binder coating. The gaps between these agglomerated Pt particles are filled with Nafion® ionomer. In comparison to Decal CCMs, Spray CCMs were fabricated using $IrO_2$ as anode CL, Pt black as the cathode CL, and 20 wt%

Table 3 Comparative table of different CCM-MEA its cell performance in AEMWEs

| S. no. | Anode | Cathode | Membrane | CCM method | Temperature (°C) | Feed | Cell performance (cell voltage and current density) | Ref. |
|---|---|---|---|---|---|---|---|---|
| 1 | $IrO_2$ | 40 wt% Pt/C | FAA-3-50 | Slurry coating | 70 | 1 M KOH | 1.9 V at 2760 mA $cm^{-2}$ | 89 |
| 2 | $NiCo_2O_4$ | $NiFe_2O_4$ | CM-PSEBS | Spray coating | 45 | 10% KOH (5 mL $min^{-1}$) | 2.2 V at 0.25 A $cm^{-2}$ | 90 |
| 3 | $IrO_2$ | 40% Pt/C | Fumasep® FAA-3-50 | Spray coating | 80 | 1 M KOH (5 mL $min^{-1}$) | 1.8 V at 1.05 A $cm^{-2}$ | 91 |
| 4 | $NiCo_2O_4$ | $NiFe_2O_4$ | CM-PSEBS-*f*-DABCO | Spray coating | 80 | 1 M KOH (50 mL $min^{-1}$) | 1.2 V at 1441.7 mA $cm^{-2}$ | 92 |
| 5 | $NiCo_2O_4$ | $NiFe_2O_4$ | CM-PSEBS-*f*-DABCO | Air brush and CNC | 45 | 1 wt% KOH | CCM-MEA: 2 V at 82 mA $cm^{-2}$; CNC-CCM-MEA: 2 V at 72 mA $cm^{-2}$ | 93 |
| 6 | Ir black | Pt/C | Benzylated HMT-PMBI | Spray coating | 60 | 1 M KOH | 1.74 V at 240 mA $cm^{-2}$ | 94 |
| 7 | $IrO_2$ | 40% Pt/C | Fumasep® FAA-3-50 | Spray coating | 60 | 1 M KOH | 2.2 V at 2.7 A $cm^{-2}$ | 95 |
| 8 | NiFe | 20 wt% Pt/C | Sustainion X37-50 | *In situ* deposition | 50 | 1 M KOH | 1.79 V at 1 A $cm^{-2}$ | 96 |
| 9 | $IrO_2$ | Pt/C | Aemion+ HLE8-25-X | Bar coating | 60 | 0.1 M KOH and 1 M KOH | 1.8 V at 1.5 A $cm^{-2}$; 1.8 V at 2 A $cm^{-2}$ | 97 |
| 10 | $IrO_2$ | 50 wt% Pt/C | Tokuyama A201 | Spray coating | 60 | 1 M KOH | 1.95 V at 2000 mA $cm^{-2}$ | 98 |
| 11 | Ni–CoO | Pt/C | QBM-2.7 | PSS method | 80 | 1 M KOH | 1.62 V at 1.0 A $cm^{-2}$ | 99 |
| 12 | $IrO_2$ | Pt/C | PBI/TPPR | Spray coating | 25 | 1 M KOH (60 mL $min^{-1}$) | 2.8 V at 0.9 A $cm^{-2}$ | 100 |
| 13 | IrOx | Pt/C | Aemion+ | Spray coating | 25 | 0.1 M KOH | 1.68 V at 1 A $cm^{-2}$ | 101 |
| 14 | $NiFe_2O_4$ | Pt/C | FAA-3-50 | Spray coating | 60 | 1 M KOH | 2.5 V at 2.0 A $cm^{-2}$ | 102 |

Note: CM-PSEBS-f-DABCO – chloromethylated polystyrene-*block*-poly(ethylene-ran-butylene)-*block*-polystyrene functionalized 1,4-diazabicyclo [2.2.2] octane; HMT-PMBI – hexamethyl-*p*-terphenyl poly(benzimidazolium); QBM – quaternized BM; PBI/TPPR – polybenzimidazole/thermoplastic phenolic resin; CNC – computer controlled ultrasonic dispersion deposition; PSS – pulsed swirl spray.

Nafion® at both electrodes, employing a direct spray deposition method. As evidenced by the SEM images in Fig. 11(e) and (f), the composition of the anode CL primarily consisted of randomly distributed small agglomerates, with the $IrO_2$ particles effectively blended with Nafion® binders. In contrast, the cathode CL exhibited larger particle agglomerates with a particle size range of 2 to 5 mm, forming a porous structure, as illustrated in Fig. 11(g) and (h). Comparative to Decal CCMs, Spray CCMs demonstrated a more even distribution of catalyst particles within the Nafion® binder, and the porous morphology of CLs is anticipated to facilitate gas transport within the CL, thereby enhancing electrolyser performance in a PEMEC relative to Decal CCMs. To ascertain which CCM fabrication method yields superior cell performance, *in situ* cell testing of Decal CCM-20% Nafion® and Spray CCM-20% Nafion® at 80 °C was conducted under identical conditions. As depicted in Fig. 11(i), Decal CCM-20%Nafion exhibited considerably lower cell voltage across the current density range of 0 to 1.5 A $cm^{-2}$, indicating smaller activation losses compared to Spray CCM-20% Nafion®. This discrepancy may be attributed to the denser anode CL of Decal CCM, which facilitates proton transport throughout the entire anode CL, thereby enhancing catalyst utilization. However, Spray CCM-20% Nafion® demonstrated superior cell performance beyond 1.5 to 2 A $cm^{-2}$. At 2 A $cm^{-2}$, the cell voltage of Spray CCM-20% Nafion was 1.984 V, representing a 38 mV reduction compared to Decal CCM-20% Nafion (2.022 V). Notably, both Decal CCM-20% Nafion® and Spray CCM-20% Nafion® exhibited stable HFR curves, indicating minimal changes in HFR values across the current density range from 0 to 2 A $cm^{-2}$ (Fig. 11(j)). The EIS plots of CCMs fabricated *via* various methods were monitored as depicted in Fig. 11(k). The corresponding ohmic resistances of Decal CCM-20% Nafion® and Spray CCM-20% Nafion® were 0.203 and 0.150 Ohm $cm^2$, respectively. Notably, the ohmic loss from Spray CCM-20% Nafion® was smaller than that of Decal CCM-20% Nafion®. Additionally, Decal CCM-20% Nafion® exhibited a second semi-circle in the EIS plot, indicative of significant mass transport losses within the cell. Conversely, Spray CCM-20% Nafion® displayed only one semi-circle, suggesting negligible mass transport losses. Furthermore, the research finds that both too low and too high ionomer contents can detrimentally affect cell performance, either by limiting proton transport and catalyst utilization or by obstructing gas transport channels and diminishing electrical conductivity, especially in the anode with noble metal oxides. This study not only addresses the technical aspects of CCM optimization but also provides a strategic pathway toward reducing the manufacturing costs of PEMECs while enhancing their efficiency. The findings advocate for the strategic regulation of Nafion® ionomer content in the anode catalyst layer as a simple yet effective approach to significantly improve PEMEC performance.

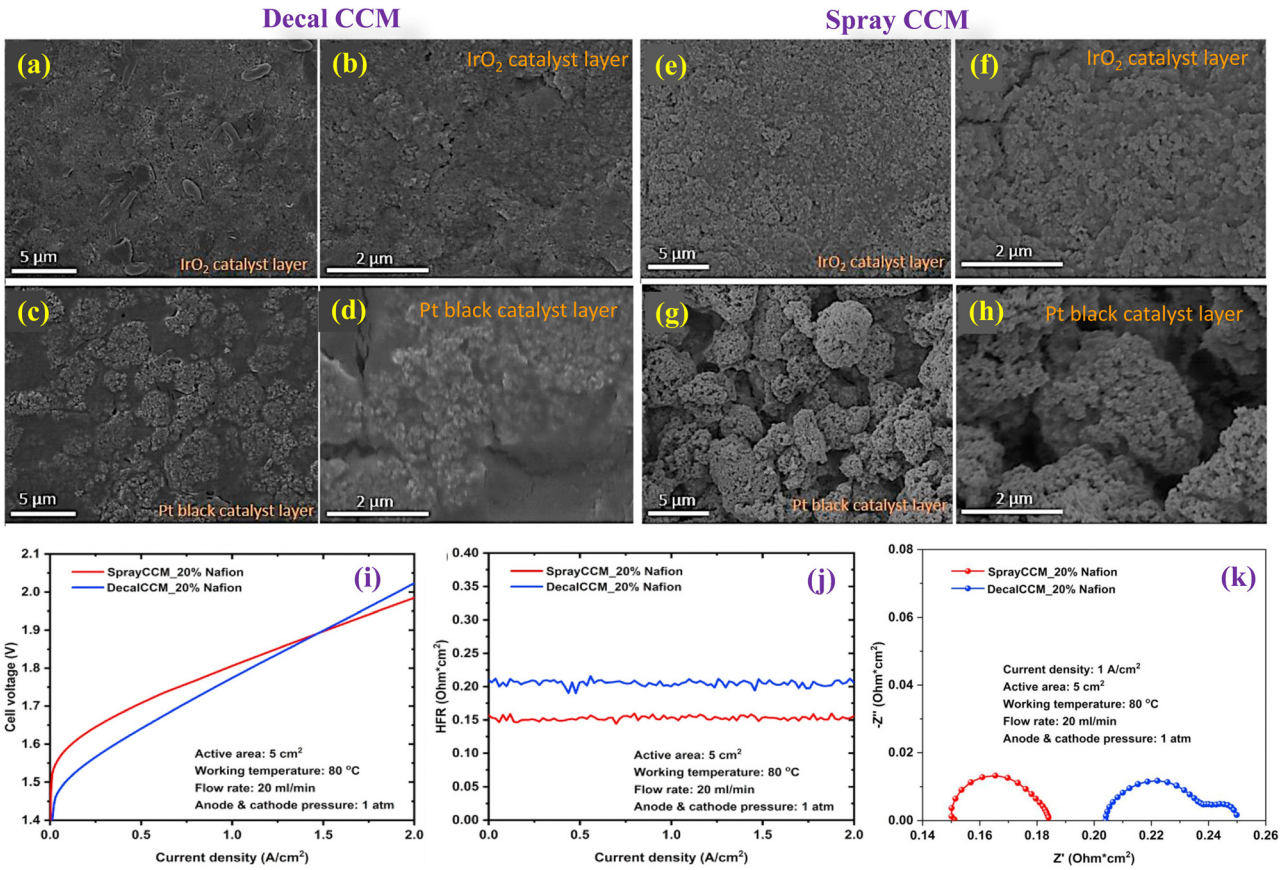


Fig. 11 SEM images of a Decal CCM (a)–(d) and Spray CCM (e)–(h); (i) polarization curves of Decal and Spray CCM; (j) HFR curves; and (k) EIS plot. Reproduced with the permission from ref. 104. Copyright 2021, Elsevier.

Fan *et al.* introduces a cost-effective approach by using a mixed metal oxide-coated Ti felt as a porous transport layer (PTL) in PEM water electrolysers.[105] This innovative method employs $IrO_2$–$RuO_2$–$TaO_x$ coating applied through thermal decomposition to enhance catalytic activity and stability while significantly reducing precious metal content to 1 mg $cm^{-2}$ in the anode catalyst layer. The coated Ti felt exhibited exceptional performance in PEM electrolyser tests, achieving a significant milestone with a single cell performance of 1.836 V at 2000 mA $cm^{-2}$ at 80 °C under ambient pressure.

Holzapfel *et al.* introduced a novel fabrication method called direct membrane deposition (DMD) for membrane electrode assemblies in PEMWE. This technique involves spray-coating the membrane directly onto a cathode electrode, a departure from traditional methods that use pre-matured membranes and aim to reduce losses associated with MEA assembly.[106] The DMD approach shows promising electrochemical performances, with reduced ohmic and mass transport losses compared to standard CCM and PTE methods. Furthermore, the study also highlights the potential for simplified manufacturing and greater design flexibility in MEA production, suggesting this method could lead to advancements in the efficiency and cost-effectiveness of hydrogen production technologies.

Sapountzi *et al.* investigated a novel vapor-phase spark ablation technique for producing CCMs in PEMWE. This method significantly reduced iridium usage-up to five times less than commercial CCMs-without compromising activity, enhancing the economic viability and sustainability for $H_2$ production.[107] The spark-ablation CCMs demonstrate robust durability over 150 hours of testing under various load profiles, highlighting their potential for long-term operational stability. Additionally, the simplified manufacturing process, which eliminates the need from complex chemical handling, presents a more environmentally, friendly and cost-effective approach to CCM production, positioning spark-ablation as a promising advancement in the scale-up of PEM electrolysis technology.

Kuhnert *et al.* studied the degradation mechanisms in PEM water electrolysers, emphasizing the adverse effects of hydrogen crossover on membrane integrity.[108] Highlighting a membrane-focused accelerated stress test (AST), the study reveals that higher temperature significantly increase hydrogen crossover, resulting in accelerated membrane degradation evidenced by increased high-frequency resistance (HFR) and fluoride emission rates (FER). These findings highlight the critical need for optimized operational conditions and advanced membrane materials to enhance the durability and reliability of PEM systems.

Wang *et al.* 2023 focused on evaluating sulfo-phenylated polyphenylene CCMs for PEM water electrolysis.[109] Utilizing sulfo-phenylated polyphenylene biphenyl (sPPB-H+) membranes alongside Nafion® D520 ionomer in the CLs, the research demonstrates a sophisticated approach to enhancing electrolysis efficiency. The Nafion® D520 ionomer was used to create the optimal balance of hydrocarbon components in the sPPB-$H^+$ membrane, which was used to make the CCMs. The CCMs were tested for performance and durability in electrolysis experiments conducted at 70 °C using deionized water. At 1 A $cm^{-2}$, sPPB-H+ based CCMs exhibited a lower operating voltage of 1.66 V compared to 1.75 V for NR112 recast membranes, indicating enhanced efficiency. Chronopotentiometry and hydrogen gas crossover studies demonstrated that sPPB-H+ membrane CCMs had significantly higher voltage increase rates (3.29 mV $h^{-1}$ for sPPB-H+ CCM-1) compared to NR112, suggesting potential durability concerns. Initially, the hydrogen gas content in the anode compartment was lower for sPPB-H+ CCMs, indicating less crossover at the beginning, but it increased over time, suggesting membrane degradation. The study emphasizes the potential for enhancing the efficiency of PEM water electrolysis through the use of sulfo-phenylated polyphenylene membranes. These membranes are effective in reducing the applied potential and gas crossover rates, but there are still areas that need improvement. The research identifies the need for more durable and efficient hydrocarbon-based CCMs for sustainable hydrogen production, highlighting the importance of balancing chemical and mechanical stability with electrochemical performance.

Rocha *et al.* explores the effect of membrane thickness and catalyst viability on the performance of PEM water electrolysers.[110] It highlights how thicker membranes, like Nafion® 117, exhibit greater ohmic overvoltage's compared to thinner ones, such as Nafion® 115, affecting efficiency. Different catalysts, including Ir black, IrOx, and $IrRuO_x$/Pt are evaluated, with $IrRuO_x$/Pt showing improved performance at lower voltages. Additionally, increased operating temperatures and hydrogen purges are shown to enhance performance by reducing activation and ohmic overvoltage's, indicating the performance of optimizing operational conditions for better electrolyser efficiency and cost-effectiveness.

T. H. Kwan *et al.* studied the development of a novel multifunctional CCM for PEMWE and intended to enhance the utilization of iridium catalysts and reduce hydrogen crossover.[111] They used Nafion® N112, N115, and N117 membranes. An electroless platinum (Pt) sublayer was subsequently deposited directly on the membrane surface to serve as a base for the iridium oxide (IrOx) catalyst layer, to enhance connectivity and reduce Ir loading. The use of IrOx over Pt sublayer *via* spray coating was implemented for the anode in the present study. Additionally, Pt/C was utilized as the cathode catalyst. This structural arrangement aimed to optimize catalyst utilization and minimize crossover to improve the overall efficiency of the electrolysis process. Fig. 12 represents the difference between the commercial CCM for water electrolysis (Fig. 12(a)) and the modified CCM (Fig. 12(c)) along with their corresponding cross-sectional SEM images (Fig. 12(b) and (d)). The SEM analysis of the modified CCMs revealed the presence of a dense and thin Pt sublayer beneath the IrOx anode catalyst layer. This sublayer was designed to reduce Ir catalyst loading and minimize hydrogen crossover. The thin Pt sublayer, with loading of approximately 130 μg $cm^{-2}$, improved the uniformity and connectivity of the IrOx layer, which may enhance the OER activity. The incorporation of a Pt sublayer resulted in a substantial decrease in crossover levels, with experimental

outcomes revealing a reduction of up to 40% in comparison to conventional CCMs. This decrease in crossover was attributed to the recombination of $H_2$ and $O_2$ within the Pt layer, thereby enhancing not only safety but also overall performance. The electrochemical performance of modified CCMs exhibited a decrease in potential of 100–200 mV at 1 A $cm^{-2}$ and 400–600 mV at 2 A $cm^{-2}$ compared to the baseline CCMs. This performance improvement was attributed to the Pt sublayer facilitating enhanced catalyst layer utilization. The incorporation of the Pt sublayer not only enhanced performance but also resulted in a decrease in in-plane resistivity, indicating reduced ohmic losses. This suggests that the novel CCM structure has the potential to improve the efficiency of electrolysis processes. The electroless Pt layers offer several advantages that enhance iridium utilization, reduce hydrogen crossover, diminish ohmic resistance, and heighten electrolysis performance. Nevertheless, there are some potential disadvantages to consider, including the added complexity and expense of incorporating an additional layer of electroless Pt, as well as the need for optimization to fully realize these benefits across varying operating conditions and membrane types.

Table 4 gives a comparative chart of the reported CCM-based PEMWE system and its performance. In summary, PEM water electrolysis with CCMs has gained traction in various industries, including renewable energy storage, transportation, and industrial processes. The current CCMs exhibited improved performance characteristics, such as higher production rates and improved durability. While challenges like cost and durability persist, ongoing research and development efforts aim to further enhance their performance and make them key enablers in the transition to the hydrogen economy.

## 11. Critical elements influencing water electrolyser performance and durability

Catalyst efficiency: the efficacy and long-term stability of the catalyst at both the anode and cathode are crucial of the performance of hydrogen and oxygen evolution reactions. Catalysts should enable quick charge transfer and possess strong resistance to corrosion in operational conditions.

Membrane conductivity and durability: the membranes, such as AEM or PEM must exhibit high ionic conductivity to reduce ohmic losses and retain their mechanical and chemical integrity under extreme acidic or alkaline conditions for prolonged periods.

Interface optimization: the junction between the membrane and catalyst layers must be finely tuned to facilitate efficient ionic transport and reduce resistance.

Mass transfer: effective movement of water to the reaction sites and the expulsion of produced gases ($H_2$ and $O_2$) are essential. Inefficient mass transfer can cause concentration overpotentials and diminish the efficiency of the system.

System architecture and integration: the structural design of the water electrolysis setup, including its flow field, current distribution, and thermal regulation, is critical for its operational performance and durability.

### 11.1. Improvement strategies of water electrolyser performance and durability Catalyst development

Pursue the research and development of new catalysts with greater activity, affordability, and durability, focusing on nanostructures,

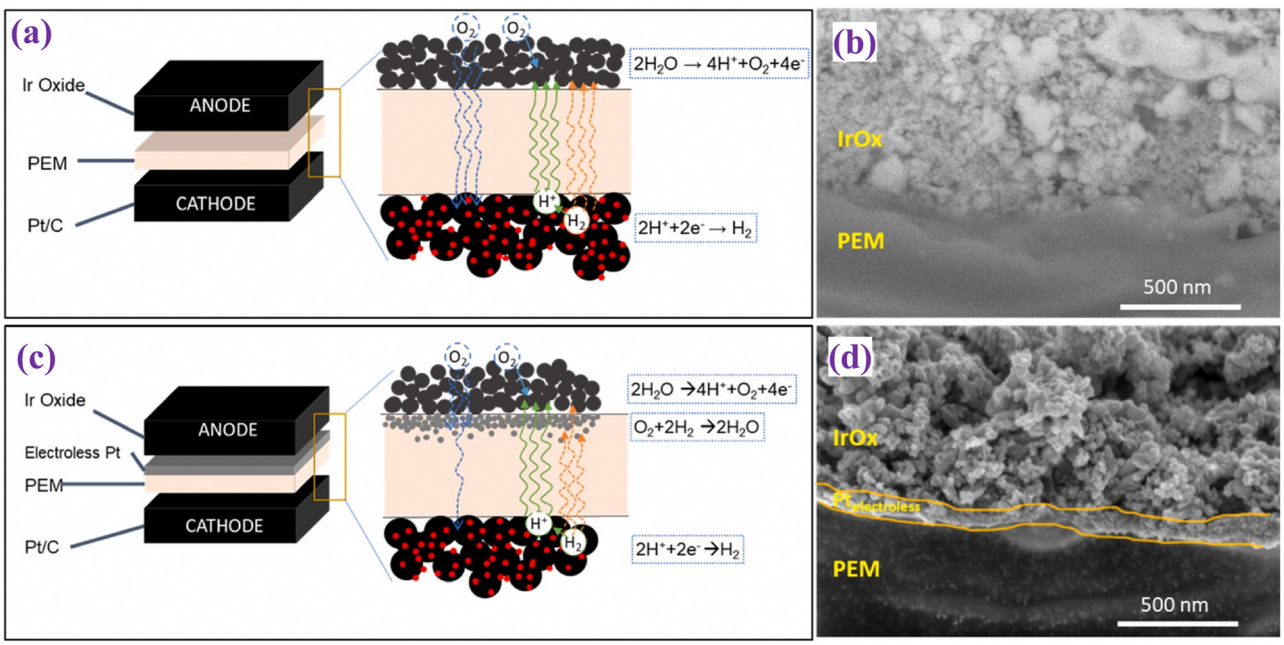


Fig. 12 (a) and (b) represent a schematic view of commercial CCM-electrolyser and SEM image, respectively; (c) and (d) schematic view of modified CCM-electrolyser and its corresponding SEM image. Reproduced with the permission from ref. 111. Copyright 2024, Elsevier.

Table 4 Comparative table of different CCM-MEA and its cell performance in PEMWEs

| S. no. | Anode | Cathode | Membrane | CCM method | Temperature (°C) | Feed | Cell performance (cell voltage and current density) | Ref. |
|---|---|---|---|---|---|---|---|---|
| 1 | Ir | Pt | Nafion® NE 1035 | Sputter etched process | 80 | DI $H_2O$ (3 mL $min^{-1}$) | 2.0 V at 4000 mA $cm^{-2}$ | 103 |
| 2 | $IrO_2$ | Pt | Nafion® 115 | Decal and direct spray deposition | 80 | DI $H_2O$ (20 mL $min^{-1}$) | 1.887 V at 2 A $cm^{-2}$ | 104 |
| 3 | Ir black | Pt | Not available | Spraying method | 80 | DI $H_2O$ (20 mL $min^{-1}$) | 1.84 V at 2000 mA $cm^{-2}$ | 105 |
| 4 | $IrO_2$ | Pt/C | Nafion® 117 | Spray coating | 80 | DI $H_2O$ | 1.95 V at 2.0 A $cm^{-2}$ | 106 |
| 5 | IrOx | Pt | Nafion® 115 | Spark ablation | 60 | DI $H_2O$ | 2 V at 790 mA $cm^{-2}$ | 107 |
| 6 | Ir | Pt/C | Nafion® 117 | Spray coating | 60 | DI $H_2O$ | 2.1 V at 2.0 A $cm^{-2}$ | 108 |
| 7 | Ir | Pt | SPPB-$H^+$ | Spray coating | 70 | DI $H_2O$ | 1.9 V at 2.4 A $cm^{-2}$ | 109 |
| 8 | $IrRuO_x$ | Pt | Nafion® 115 | Spray coating | 80 | DI $H_2O$ | 1.85 V at 2.4 A $cm^{-2}$ | 110 |
| 9 | IrOx | Pt/C | Nafion® N115 | Spray coating | 25 | DI $H_2O$ | 2.0 V at 2 A $cm^{-2}$ | 111 |

bimetallic alloys, or non-precious metal catalysts for cost-effective high performance.

Membrane advancements: seek out new membrane materials with superior conductivity, thermal robustness, and chemical resistance. The exploration of hybrid or composite membranes could also enhance performance and lifespan.

CCM interface enhancement: improve the interface between the catalyst layer and the membrane through better coating methods, ensuring uniform catalyst distribution, and optimal catalyst and ionomer loading.

Engineering innovations: refine the electrolysis cell design, particularly the flow field arrangement, to boost mass transport and thermal management, thus mitigating concentration gradients, enhancing reaction kinetics, and increasing system efficiency.

Operational optimization: develop control strategies for the electrolysis system to operate under ideal conditions, adjusting factors such as temperature, pressure, and current density to optimize efficiency and longevity.

System integration: for large-scale hydrogen production, combine water electrolysis systems with renewable energy sources like solar or wind power to achieve a sustainable and economically viable green hydrogen supply.

In summary, the advancement of water electrolysis system performance and stability requires a comprehensive strategy encompassing material innovation, particularly in catalyst and membrane technology, along with engineering and operational refinements to maximize the system's efficiency and life span.

# 12. Mechanism of poor polarization behavior and poor reproducibility of CCM

The poor polarization behavior and reproducibility in CCMs for water electrolysis can be attributed to several factors, which required detailed analysis.[112,113]

## 12.1. Mechanism behind poor polarization behavior

**(i) Catalyst layer degradation.** Over time, the catalyst layer within the CCM can degrade due to the harsh operating conditions, including high potentials and corrosive environments. This degradation can lead to a decrease in the active surface area of the catalyst, resulting in increased polarization losses.

**(ii) Membrane deterioration.** The membrane in CCMs, particularly in PEMWE, can thin out and form pinhole over extended use, which increase gas crossover and electrical resistance, leading to higher polarization voltages.

**(iii) Interfacial issues.** Poor interfacial contact between the membrane and the catalyst layer can cause increased charge transfer resistance. Inhomogeneous distribution of catalyst particles and ionomer within the catalyst layer can result in non-uniform current density distribution and localized hot spots, exacerbating polarization losses.

**(iv) Mass transport limitations.** Inefficient removal of gases ($H_2$ and $O_2$) from the reaction sites can lead to mass transport limitations, further increasing polarization. The design of gas diffusion layers and the overall water management in the system play crucial roles in minimizing these effects.

## 12.2. Mechanism behind poor reproducibility

**(i) Manufacturing variability.** The reproducibility issues in CCMs can often be traced back to variations in the manufacturing process, including the catalyst loading, distribution uniformity, and membrane thickness. Minor deviations in these parameters can lead to significant performance disparities.

**(ii) Catalyst degradation and contamination.** Variability in the long-term stability of the catalyst, due to sintering or contamination, can lead to inconsistent performance. Different patches of catalysts may also have varying levels of impurities, affecting their performance and reproducibility.

**(iii) Membrane inconsistencies.** Variations in membrane properties, such as ion exchange capacity, thickness, and mechanical strength, can lead to inconsistent performance. The interaction between the membrane and the catalyst layer is critical for ensuring uniform ion transport and minimizing performance variability.

# 13. Conclusions and future perspectives

The comprehensive analysis of CCM underscores their pivotal role in the evolution of sustainable hydrogen production technologies. This review has dissected the multifaceted

dimensions of CCMs, including their design, manufacturing processes, catalyst choices, and the strategies to augment their performance and durability. The synergy between the membrane materials, catalyst layers, and supporting structures is crucial, necessitating an integrated approach to refine CCMs for enhanced electrochemical performance and operational longevity.

Looking forward, the specific future directions of CCMs presents both exciting opportunities and challenges. Here are key areas for further exploration.

Material innovations: future research should prioritize the discovery and application of innovative catalyst materials that reduce or eliminate the dependence of noble metals. Emphasis or earth-abundant, non-precious metal catalysts with high activity, selectivity, and stability will be vital. Detailed studies on the degradation mechanisms of these materials under operational stresses will help in enhancing their durability and efficiency.

Advanced manufacturing: the development of cutting-edge fabrication methods is essential. Techniques like atomic layer deposition, 3D printing, and electrospinning could offer unprecedented control over the nanostructure of CCM components, optimizing their functionality and reducing production costs.

Operational excellence: investigate the effect of operating conditions (temperature, pressure, and electrolyte concentration) on CCM performance and stability. Developing advanced diagnostic tools and techniques to monitor and control these parameters in real-time will enhance the system's efficiency and operational life.

Renewable energy integration: explore innovative ways to integrate CCM-based electrolysers with renewable energy systems. Research on adaptive control systems that can dynamically adjust electrolyser operations based on fluctuating renewable energy outputs will be crucial for developing efficient, grid-independent hydrogen production systems.

By focussing on these areas, the research community and industry can collaboratively advance CCM technology from laboratory research to commercial reality, making it a cornerstone of the future hydrogen economy. The successful deployment of CCMs in water electrolysis systems will be instrumental in achieving a sustainable, low-carbon energy landscape.

## Conflicts of interest

Authors declare no conflict of interest.

## Acknowledgements

The researchers at the Green Hydrogen Lab (UQTR's Hydrogen Research Institute) would like to acknowledge the support of the Natural Sciences and Engineering Research Council of Canada (NSERC) Tier 1 Canada Research Chair in Green Hydrogen Production, the Québec Ministère de l'Économie, de l'Innovation et de l'Énergie (MEIE) [Développement de catalyseurs et d'électrodes innovants, à faibles co û ts, performants et durables pour la production d'hydrogène vert, funding reference number 00393501], and Innergex Renewable Energy Inc. for the Innergex Research Chair in Renewable Hydrogen Production.

## References

1 K. T. Møller, T. R. Jensen, E. Akiba and H. Li, *Prog. Nat. Sci. Mater. Int.*, 2017, **27**, 34–40.
2 S. Dunn, *Int. J. Hydrogen Energy*, 2002, **27**, 235–264.
3 A. Ursúa, L. M. Gandía and P. Sanchis, *Proc. IEEE*, 2012, **100**(2), 410–426.
4 L.-F. Gu, J.-J. Chen, T. Zhou, X.-F. Lu and G.-R. Li, *Nanoscale*, 2020, **12**, 11201.
5 Z. Pei, X. F. Lu, H. Zhang, Y. Li, D. Luan and X. W. Lou, *Angew. Chem., Int. Ed.*, 2022, **61**, e202207537.
6 X. Sun, S. Wang, Y. Hou, X. F. Lu, J. Zhang and X. Wang, *J. Mater. Chem. A*, 2023, **11**, 13089.
7 O. F. Aldosari, I. Hussain and Z. Malaibari, *J. Energy Chem.*, 2023, **80**, 658–688.
8 N. Logeshwaran, S. Vijayapradeep, A. R. Kim, P. Sampath, S. Ramakrishnan, M. B. Poudel, D. H. Kim and D. J. Yoo, *J. Energy Chem.*, 2023, **86**, 167–179.
9 J. R. Deiman, *Water*, 2010, **2**, 4–9.
10 P. Millet and S. Grigoriev, Water electrolysis technologies, *Renewable Hydrogen Technologies: Production, Purification, Storage, Applications and Safet*, 2013, ch. 2, pp. 19–41.
11 F. E. Senftle, J. R. Grant and F. P. Senftle, *Electrochim. Acta*, 2010, **55**(5), 148–153.
12 Z. D. Wei, M. B. Ji, S. G. Chen, Y. Liu, C. X. Sun, G. Z. Yin, P. H. Shen and S. H. Chan, *Electrochim. Acta*, 2007, **52**, 3323–3329.
13 C. Wang, L. Yu, F. Yang and L. Feng, *J. Energy Chem.*, 2023, **87**, 144–152.
14 C. Liu, Z. Geng, X. Wang, W. Liu, Y. Wang, Q. Xia, W. Li, L. Jin and C. Zhang, *J. Energy Chem.*, 2024, **90**, 348–369.
15 J. Chi and H. Yu, *Chin. J. Catal.*, 2018, **39**, 390–394.
16 T. Lim and S. K. Kim, *Chem. Eng. J.*, 2022, **433**, 133681.
17 J. C. Ganley, *Int. J. Hydrogen Energy*, 2009, **34**, 3604–3611.
18 H. Tüysüz, *Acc. Chem. Res.*, 2024, **57**, 558–567.
19 A. J. Appleby, G. Crepy and J. Jacquelin, *Int. J. Hydrogen Energy*, 1978, **3**, 21–37.
20 K. Zeng and D. Zhang, *Prog. Energy Combust. Sci.*, 2010, **36**, 307–326.
21 H. Wendt and H. Hofmann, *J. Appl. Electrochem.*, 1989, **19**, 605–610.
22 V. Rosa, *Int. J. Hydrogen Energy*, 1995, **20**, 697–700.
23 W. A. Hu, *Int. J. Hydrogen Energy*, 1997, **22**, 621–623.
24 C. K. Kjartansdóttir, L. P. Nielsen and P. Møller, *Int. J. Hydrogen Energy*, 2013, **38**, 8221–8231.
25 J. O. Jenson, V. Bandur, N. J. Bjerrum, S. H. Jensen, S. Ebbesen, M. Mogensen, N. Tophøj and L. Yde, *Pre-Investigation of water electrolysis*, 2008, pp. 195.
26 D. Ferrero, A. Lanzini, M. Santarelli and P. Leone, *Int. J. Hydrogen Energy*, 2013, **38**, 3523–3536.

27 P. Millet, R. Ngameni, S. A. Grigoriev, N. Mbemba, F. Brisset, A. Ranjbari and C. Etiévant, *Int. J. Hydrogen Energy*, 2010, **35**, 5043–5052.
28 R. B. Sutherland, Thesis, *Performance of different proton exchange membrane water electrolyser components*, North-West University, Potchefstroom, South Africa, 2012.
29 P. Millet, N. Mbemba, S. A. Grigoriev, V. N. Fateev, A. Aukauloo and C. Etiévant, *Int. J. Hydrogen Energy*, 2011, **36**, 4134–4142.
30 J. Rossmeisl, Z. W. Qu, H. Zhu, G. J. Kroes and J. K. Nørskov, *J. Electroanal. Chem.*, 2007, **607**, 83–89.
31 *Hydrogen production by electrolysis*, ed. A. Godula-Jopek, Wiley-VCH, Weinheim, 2015.
32 D. Bessarabov, H. Wang and N. Zhao, *PEM electrolysis for hydrogen production*, CRC Press, Boca Ration, 2015.
33 J. R. Varcoe, P. Atanassov, D. R. Dekel, A. M. Herring, M. A. Hickner, P. A. Kohl, A. R. Kucernak, W. E. Mustain, K. Nijmeijer, K. Scott, T. Xu and L. Zhuang, *Energy Environ. Sci.*, 2014, **7**, 3135–3191.
34 Y. Leng, G. Chen, A. J. Mendoza, T. B. Tighe, M. A. Hickner and C.-Y. Wang, *J. Am. Chem. Soc.*, 2012, **134**, 9054–9057.
35 X. Wang, A. M. Thomas and R. G. H. Lammertink, *ACS Appl. Mater. Interfaces*, 2024, **16**(2), 2593–2605.
36 C. C. Pavel, F. Cecconi, C. Emiliani, S. Santiccioli, A. Scaffidi, S. Catanorchi and M. Comotti, *Angew. Chem., Int. Ed.*, 2014, **53**, 1378–1381.
37 W. Xu and K. Scott, *Int. J. Hydrogen Energy*, 2010, **35**, 12029–12037.
38 A. Brisse, J. Schefold and M. Zahid, *Int. J. Hydrogen Energy*, 2008, **33**, 5375–5382.
39 M. Liang, B. Yu, M. Wen, J. Chen, J. Xu and Y. Zhai, *J. Power Sources*, 2009, **190**, 341–345.
40 P. Moçoteguy and A. Brisse, *Int. J. Hydrogen Energy*, 2013, **38**, 15887–15902.
41 J. Rostrup-Nielsen and L. J. Christiansen, Concepts in Syngas Preparation, *Catalytic Science Series*, Imperial College Press, London, UK, 2011.
42 M. El-Shafie, *Res. Eng.*, 2023, **20**, 101426.
43 N. S. Hassan, A. A. Jalil, S. Rajendran, N. F. Khusnun, M. B. Bahari, A. Johari, M. J. Kamaruddin and M. Ismail, *Int. J. Hydrogen Energy*, 2024, **52**(Part B), 420–441.
44 H. Lange, A. Klose, W. Lippmann and L. Urbas, *Int. J. Hydrogen Energy*, 2023, **48**(42), 15771–15783.
45 H. Lv, J. Chen, W. Zhou, X. Shen and C. Zhang, *Renewable Sustainable Energy Rev.*, 2023, **183**, 113394.
46 Z. Zou, K. Dastafkan, Y. Shao, C. Zhao and Q. Wang, *Int. J. Hydrogen Energy*, 2024, **51**(Part A), 667–684.
47 C. Daoudi and T. Bounahmidi, *Int. J. Hydrogen Energy*, 2024, **49**(Part C), 646–667.
48 M. Bonanno, K. Müller, B. Bensmann, R. Hanke-Rauschenbach, D. Aili, T. Franken, A. Chromik, R. Peach, A. T. S. Freiberg and S. Thiele, *Adv. Mater. Technol.*, 2024, **9**, 2300281.
49 D. Niblett, M. Delpisheh, S. Ramakrishnan and M. Mamlouk, *J. Power Sources*, 2024, **592**, 233904.
50 S. Shiva Kumar and H. Lim, *Sustainable Energy Fuels*, 2023, **7**, 3560.
51 L. Wan, Z. Xu, Q. Xu, M. Pang, D. Lin, J. Liu and B. Wang, *Energy Environ. Sci.*, 2023, **16**, 1384.
52 D. S. Falcão, *Energies*, 2023, **16**, 943.
53 R. Vinodh, S. S. Kalanur, S. K. Natarajan and B. G. Pollet, *Polymers*, 2023, **15**(9), 2144.
54 C. Liu, K. Wippermann, M. Rasinski, Y. Suo, M. Shviro, M. Carmo and W. Lehnert, *ACS Appl. Mater. Interfaces*, 2021, **13**(14), 16182–16196.
55 L. Wan, Z. Xu, Q. Xu, M. Pang, D. Lin, J. Liu and B. Wang, *Energy Environ. Sci.*, 2023, **16**, 1384.
56 S. A. Lee, S. E. Jun, S. H. Park, K. C. Kwon, J. H. Kang, M. S. Kwon and H. W. Jang, *EES Catal.*, 2024, **2**, 49.
57 D. Chanda, J. Hnat, A. S. Dobrota, I. A. Pasti, M. Paidar and K. Bouzek, *Phys. Chem. Chem. Phys.*, 2015, **17**, 26864–26874.
58 D. Chanda, J. Hnat, M. Paidar, J. Schauer and K. Bouzek, *J. Power Sources*, 2015, **285**, 217–226.
59 M. R. Kraglund, D. Aili, K. Jankova, E. Christensen, Q. Li and J. O. Jensen, *J. Electrochem. Soc.*, 2016, **163**, F3125–F3131.
60 D. Burnat, M. Schlupp, A. Wichser, B. Lothenbach, M. Gorbar, A. Züttel and U. F. Vogt, *J. Power Sources*, 2015, **291**, 163–172.
61 M. Carmo, D. L. Fritz, J. Mergel and D. Stolten, *Int. J. Hydrogen Energy*, 2013, **38**, 4901–4934.
62 A. Lindermeir, G. Rosenthal, U. Kunz and U. Hoffmann, *J. Power Sources*, 2004, **129**, 180–187.
63 I.-S. Park, W. Li and A. Manthiram, *J. Power Sources*, 2010, **195**, 7078–7082.
64 M. Bühler, P. Holzapfel, D. McLaughlin and S. Thiele, *J. Electrochem. Soc.*, 2019, **166**, F1070–F1078.
65 P. Millet, D. Dragoe, S. Grigoriev, V. Fateev and C. Etievant, *Int. J. Hydrogen Energy*, 2009, **34**(11), 4974–4982.
66 L. Wan, M. Pang, J. Le, Z. Xu, H. Zhou, Q. Xu and B. Wang, *Nat. Commun.*, 2022, **13**, 7956.
67 Y. Shi, Z. Lu, L. Guo and C. Yan, *Int. J. Hydrogen Energy*, 2017, **42**, 26183–26191.
68 S. Koch, L. Metzler, S. K. Kilian, P. A. Heizmann, F. Lombeck, M. Breitwieser and S. Vierrath, *Adv. Sustainable Syst.*, 2022, **7**, 2200332.
69 M. S. Wilson and S. Gottesfeld, *J. Appl. Electrochem.*, 1992, **22**(1), 1–7.
70 J. H. Cho, J. M. Kim, J. Prabhuram, S. Y. Hwang, D. J. Ahn, H. Y. Ha and S.-K. Kim, *J. Power Sources*, 2009, **187**(2), 378–386.
71 M. S. Saha, D. K. Paul, B. A. Peppley and K. Karan, *Electrochem. Commun.*, 2010, **12**(3), 410–413.
72 G. Bender, T. A. Zawodzinski and A. P. Saab, *J. Power Sources*, 2003, **124**, 114.
73 S. Q. Song, Z. X. Liang, W. J. Zhou, G. Q. Sun, Q. Xin, V. Stergiopoulos and P. Tsiakaras, *J. Power Sources*, 2005, **145**, 495.
74 W. Wang, S. Chen, J. Li and W. Wang, *Int. J. Hydrogen Energy*, 2015, **40**(13), 4649–4658.
75 C. Xu, L. Ma, J. Li, W. Zhao and Z. Gan, *Int. J. Hydrogen Energy*, 2012, **37**(4), 2985–2992.

76 J. Xie, K. L. More, T. A. Zawodzinski and W. H. Smith, *J. Electrochem. Soc.*, 2004, **151**, A1841–A1846.
77 S. Zhang, Z. Wang, R. Zhang, Y. He and K. Cen, *Int. J. Hydrogen Energy*, 2023, **48**(91), 35463–35476.
78 E. T. Ojong, J. T. H. Kwan, A. Nouri-Khorasani, A. Bonakdarpour, D. P. Wilkinson and T. Smolinka, *Int. J. Hydrogen Energy*, 2017, **42**, 25831–25847.
79 Y. S. Park, J. Yang, J. Lee, M. J. Jang, J. Jeong, W.-S. Choi, Y. Kim, Y. Yin, M. H. Seo, Z. Chen and S. M. Choi, *Appl. Catal., B*, 2020, **278**, 119276.
80 W. W. Guo, J. Kim, H. Kim and S. H. Ahn, *Int. J. Energy Res.*, 2021, **45**, 1918–1931.
81 M. K. Cho, H.-Y. Park, S. Choe, S. J. Yoo, J. Y. Kim, H.-J. Kim, D. Henkensmeier, S. Y. Lee, Y.-E. Sung and H. S. Park, *J. Power Sources*, 2017, **347**, 283–290.
82 P. Lettenmeier, S. Kolb, N. Sata, A. Fallisch, L. Zielke, S. Thiele, A. S. Gago and K. A. Friedrich, *Energy Environ. Sci.*, 2017, **10**, 2521–2533.
83 T. Malkow, A. Pilenga and G. Tsotridis, EU harmonised test procedure: electrochemical impedance spectroscopy for water electrolysis cells, Publications Office of the European Union, 2018.
84 T. Audichon, E. Mayousse, S. Morisset, C. Morais, C. Comminges, T. W. Napporn and K. B. Kokoh, *Int. J. Hydrogen Energy*, 2014, **39**, 16785–16796.
85 F. Razmjooei, T. Morawietz, E. Taghizadeh, E. Hadjixenophontos, L. Mues, M. Gerle, B. D. Wood, C. Harms, A. S. Gago, S. A. Ansar and K. A. Friedrich, *Joule*, 2021, **5**, 1776–1799.
86 J. Wei, M. Zhou, A. Long, Y. Xue, H. Liao, C. Wei and Z. J. Xu, *Nano-Micro Lett.*, 2018, **10**, 1–15.
87 S. Siracusano, S. Trocino, N. Briguglio, V. Baglio and A. S. Aricò, *Mater.*, 2018, **11**, 1368.
88 M. Maier, K. Smith, J. Dodwell, G. Hinds, P. R. Shearing and D. J. L. Brett, *Int. J. Hydrogen Energy*, 2022, **47**, 30–56.
89 J. E. Park, H. E. Bae, M. Karuppannan, K. M. Oh, O. J. Kwon, Y.-H. Cho and Y.-E. Sung, *J. Ind. Eng. Chem.*, 2022, **109**, 453–460.
90 J. Hnat, M. Plevova, R. A. Tufa, J. Zitka, M. Paidar and K. Bouzek, *Int. J. Hydrogen Energy*, 2019, **44**, 17493–17504.
91 I. Gatto, A. Capri, C. L. Vecchio, S. Zignani, A. Patti and V. Baglio, *Int. J. Hydrogen Energy*, 2023, **48**, 11914–11921.
92 K. Lou, L. Xia, J. Friedrich and M. Shviro, *Int. J. Hydrogen Energy*, 2024, **49**, 591–603.
93 M. Plevova, J. Hnat, J. Zitka, L. Pavlovec, M. Otmar and K. Bouzek, *J. Power Sources*, 2022, **539**, 231476.
94 B. Chen, P. Mardle and S. Holdcroft, *J. Power Sources*, 2022, **550**, 232134.
95 A. Martinez-Lazaro, A. Caprì, I. Gatto, J. Ledesma-García, N. Rey-Raap, A. Arenillas, F. I. Espinosa-Lagunes, V. Baglio and L. G. Arriaga, *J. Power Sources*, 2023, **556**, 232417.
96 T. H. Kong, P. Thangavel, S. Shin, S. Kwon, H. Choi, H. Lee, N. Park, J. J. Woo and Y. Kwon, *ACS Energy Lett.*, 2023, **8**, 4666–4673.
97 S. Koch, L. Metzler, S. K. Kilian, P. A. Heizmann, F. Lombeck, M. Breitwieser and S. Vierrath, *Adv. Sustainable Syst.*, 2023, **7**, 2200332.
98 A. Kiessling, J. C. Fornaciari, G. Anderson, X. Peng, A. Gerstmayr, M. Gerhardt, S. McKinney, A. Serov, A. Z. Weber, Y. S. Kim, B. Zulevi and N. Danilovic, *J. Electrochem. Soc.*, 2022, **169**, 024510.
99 Y. Ozawa, T. Iwataki, M. Uchida, K. Kakinuma and K. Miyatake, *J. Mater. Chem. A*, 2023, **11**, 19925.
100 Z. Qiu, L. Wang, M. He, P. Zhang, H. Li, Y. Yun and T. Zhao, *J. Mater. Chem. A*, 2023, **11**, 24338.
101 S. Koch, P. A. Heizmann, S. K. Kilian, B. Britton, S. Holdcroft, M. Breitwieser and S. Vierrath, *J. Mater. Chem. A*, 2021, **9**, 15744.
102 A. Caprì, I. Gatto, C. L. Vecchio, S. Trocino, A. Carbone and V. Baglio, *ChemElectroChem*, 2023, **10**, e202201056.
103 T. Hrbek, P. Kus, Y. Yakovlev, J. Novakova, Y. Lobko, I. Khalakhan, V. Matolın and I. Matolınova, *Int. J. Hydrogen Energy*, 2020, **45**, 20776–20786.
104 Z. Xie, S. Yu, G. Yang, K. Li, L. Ding, W. Wang and F.-Y. Zhang, *Int. J. Hydrogen Energy*, 2021, **46**, 1155–1162.
105 Z. Fan, H. Yu, G. Jiang, D. Yao, S. Sun, J. Chi, B. Qin and Z. Shao, *Int. J. Hydrogen Energy*, 2022, **47**, 18963–18971.
106 P. Holzapfel, M. Bühler, C. V. Pham, F. Hegge, T. Böhm, D. McLaughlin, M. Breitwieser and S. Thiele, *Electrochem. Commun.*, 2020, **110**, 106640.
107 F. M. Sapountzi, M. Lavorenti, W. Vrijburg, S. Dimitriadou, B. T. Pueschel, P. Thüne, H. Niemantsverdriet, T. V. Pfeiffer and M. N. Tsampas, *Catalysts*, 2022, **12**, 1343.
108 E. Kuhnert, M. Heidinger, D. Sandu, V. Hacker and M. Bodner, *Membranes*, 2023, **13**, 348.
109 X. Wang, P. Mardle, M. Adamski, B. Chen and S. Holdcroft, *J. Electrochem. Soc.*, 2023, **170**, 024502.
110 A. G. Rocha, R. Ferreira, D. Falcão and A. M. F. R. Pinto, *Energies*, 2022, **15**, 7937.
111 J. T. H. Kwan, L. Daniel, W. J. Wang, K. L. W. Yao, D. S. Shehata and D. P. Wilkinson, *J. Power Sources*, 2024, **591**, 233872.
112 T. A. Berhe, W.-N. Su, C.-H. Chen, C.-J. Pan, J.-H. Cheng, H.-M. Chen, M.-C. Tsai, L.-Y. Chen, A. A. Dubale and B.-J. Hwang, *Energy Environ. Sci.*, 2016, **9**, 323–356.
113 R.-T. Liu, Z.-L. Xu, F.-M. Li, F.-Y. Chen, J.-Y. Yu, Y. Yan, Y. Chen and B. Y. Xia, *Chem. Soc. Rev.*, 2023, **52**, 5652–5683.